The Canadian Mineralogist
Vol. 38, pp. 1347-1370 (2000)

DIAMOND FROM THE GUANIAMO AREA, VENEZUELA*

FELIX V. KAMINSKY§

KM Diamond Exploration Ltd., 815 Evelyn Drive, West Vancouver, British Columbia V7T 1J1, Canada, and GEMOC National Key Centre, Department of Earth and Planetary Sciences, Macquarie University, Sydney, NSW 2109, Australia

OLGA D. ZAKHARCHENKO

Institute of Diamonds, Russian Academy of Natural Sciences, 155-5/10 Litovskii Boulevard, Moscow 117593, Russia

WILLIAM L. GRIFFIN

GEMOC National Key Centre, Department of Earth and Planetary Sciences, Macquarie University, Sydney, NSW 2109, Australia

DOMINIC M. DeR. CHANNER

Guaniamo Mining Company, Centro Gerencial Mohedano, Cruce Av. Mohedano, Urb. La Castellana, Caracas, Venezuela

GALINA K. KHACHATRYAN-BLINOVA

Institute of Diamonds, Russian Academy of Natural Sciences, 155-5/10 Litovskii Boulevard, Moscow 117593, Russia

Abstract

More than 5,000 diamond crystals (or fragments) from kimberlite sills and placer deposits in the Guaniamo area of Venezuela have been characterized in terms of morphology, internal structure, carbon isotopic composition, syngenetic mineral inclusions, and the abundance and aggregation state of nitrogen. Ours is the first comprehensive mineralogical study of diamond from the Guaniamo area. About 50% of the crystals are resorbed dodecahedral forms; octahedra are the next most common form. In most cases, the diamond is colorless; 55–90% show radiation-induced pigmentation. About 20% of the stones have very low N contents (Type II); the remainder belong to the transitional IaAB type, with B > A. Ninety-three mineral inclusions were extracted from 77 crystals or fragments of diamond and analyzed by electron microprobe and LAM–ICP–MS to establish their trace-element compositions and the pressures and temperatures of diamond crystallization. In all, 86% of the diamond samples contain inclusions of the eclogitic paragenesis, represented by garnet, omphacite, rutile, ilmenite, pyrrhotite, and probable coesite. Inclusions indicative of the peridotite paragenesis are pyrope, chromian spinel and olivine. One inclusion of ferroan periclase may indicate a lower-mantle origin. The $\delta^{13}C$ of 108 diamond samples ranges from –3.2‰ to –28.7‰, but most stones have $\delta^{13}C$ ≤10‰. We contend that in large part, the diamond in placers in the Guaniamo area was derived from the Guaniamo kimberlite sills. P–T estimates on mineral inclusions suggest that most originated near the base of the lithosphere (T 1200–1300°C); this zone may contain a substantial proportion of eclogite formed by subduction of crustal material. The very high proportion of diamond derived from an eclogitic association in the Guaniamo deposits, and several features of the mineral inclusions trapped in diamond, show striking parallels to the Argyle deposit of Australia. Both deposits occur within cratons that have experienced extensive Proterozoic tectonothermal activity.

Keywords: diamond, carbon isotope, nitrogen, mineral inclusions, eclogitic association, Guaniamo, Venezuela.

Sommaire

Nous avons caractérisé plus de 5,000 cristaux (ou fragments) de diamant provenant de filons-couches de kimberlite et de dépôts alluvionnaires dans la région de Guaniamo, au Vénézuela, selon leur morphologie, leur structure interne, la composition isotopique du carbone, leurs inclusions minérales syngénétiques, et l'abondance et l'état d'agrégation de l'azote. Ce travail

---

* Publication No. 213 of the ARC National Key Centre for Geochemical Evolution and Metallogeny of Continents (GEMOC).

§ *E-mail address*: felixvkaminsky@cs.com

constitue la première étude minéralogique compréhensive du diamant de la région de Guaniamo. Environ 50% des cristaux ont une forme dodécaédrique résorbée; l'octaèdre est la deuxième forme la plus courante. Dans la plupart des cas, le diamant est incolore; entre 55 et 90% des échantillons font preuve d'une pigmentation due à une irradiation. Environ 20% des pierres contiennent une très faible teneur en azote (type II); le reste fait partie de la catégorie transitionnelle IaAB, avec B > A. Nous avons extrait quatre-vingt treize inclusions minérales de 77 cristaux ou fragments de diamant, et nous les avons analysé avec une microsonde électronique et un plasma à couplage inductif avec spectrométrie de masse, l'instrument étant équipé pour ablation au laser, afin d'établir les teneurs en éléments traces et la pression et la température de cristallisation du diamant. En tout, 86% des échantillons de diamant contiennent des inclusions typiques d'une paragenèse éclogitique, représentée par le grenat, l'omphacite, le rutile, l'ilménite, la pyrrhotite et, probablement, la coesite. Les inclusions indicatives d'un assemblage péridotitique sont le pyrope, le spinelle chromifère et l'olivine. Une seule inclusion de périclase ferreuse indiquerait une origine très profonde dans le manteau. La valeur $\delta^{13}C$ de 108 cristaux ou fragments de diamant définit un intervalle entre –3.2‰ et –28.7‰, mais dans la plupart des cas, $\delta^{13}C$ est inférieur ou égal à 10‰. A notre avis, la plupart du diamant alluvionnaire de la région de Guaniamo provient des filons-couches de kimberlite. D'après les estimations géobarothermométriques fondées sur les inclusions minérales, la source du diamant serait en général près de la base de la couche lithosphérique, à une température entre 1200 et 1300°C; cette zone pourrait bien contenir un volume important d'éclogite à cause de la subduction de roches de la croûte. La proportion importante du diamant à Guaniamo ayant une origine éclogitique, ainsi que plusieurs aspects des inclusions minérales piégées, constituent des points de ressemblance frappants avec le gisement d'Argyle en Australie. Dans les deux cas, il s'agit de gisements situés dans un milieu cratonique ayant subi une activité tectonothermale protérozoïque importante.

(Traduit par la Rédaction)

Mots-clés: diamant, isotopes de carbone, azote, inclusions minérales, association éclogitique, Guaniamo, Vénézuela.

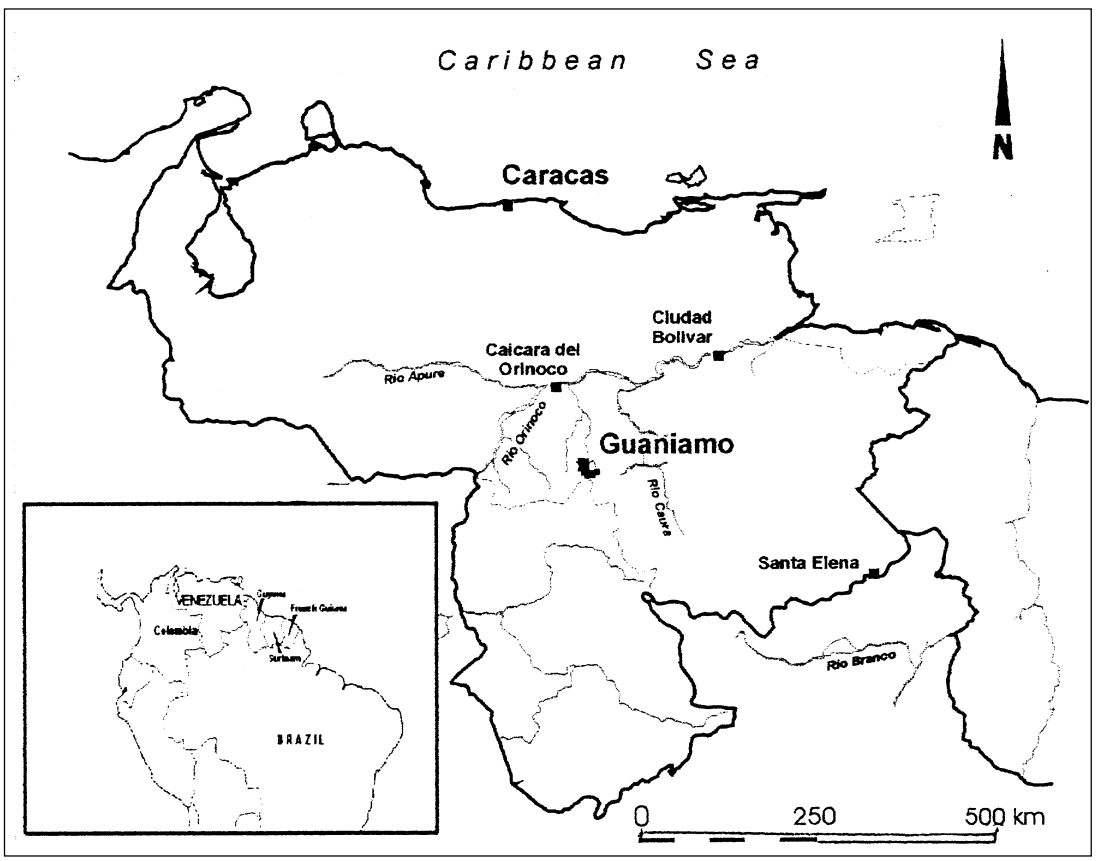

FIG. 1. Location of the Guaniamo area.

INTRODUCTION

The Guaniamo area, located in western Bolivar State, Venezuela, is one of the most promising diamondiferous areas in South America (Fig. 1). Diamond has been mined there since it was discovered in the alluvium of the Quebrada Grande River and its tributaries in 1968 (Curtis 1975, Baptista & Svisero 1978). According to official data, the placer deposits have produced approximately 15 million carats of diamond, but the actual production may have reached 25–30 million carats. Stones of up to 60 carats have been reported.

The Cuchivero province of the Guayana Shield, which includes the Guaniamo area, is dominated by felsic volcanic rocks of the Caicara Formation, with associated granitic intrusions emplaced around 1.9–1.7 Ga, and followed by intense mafic magmatism and rifting around 1.6 Ga (Mendoza 1972, Sidder & Mendoza 1995). Granites related to the Parguaza episode were emplaced at 1.55–1.42 Ga, and lamprophyre dykes intruded at 870 Ma (Nixon *et al.* 1992).

It was originally accepted that the 1.7–1.9 billion-year-old Roraima sediments were the source of the Guaniamo diamond placer deposits (Reid 1972), but in 1982 diamondiferous kimberlites were discovered within the Quebrada Grande River basin (Nixon 1988, Nixon *et al*. 1992, 1995). About 30 kimberlite localities are now known within the 10 × 6 km area of the Quebrada Grande. Initially they were described as dykes, veins, small pipes and stocks. They are now known to have formed a system of layered kimberlite sills, dipping flatly to the northeast at 5–20° (Channer *et al*. 1998). Nine sills 0.1–3 m thick (Fig. 2) have been traced for 1–12 km along Quebrada Grande and up to 1 km eastward. Their thickness varies, and they undulate. The undulation of the sills may be original and not caused by later tectonic events, although minor offsets due to brittle faulting are possible. The kimberlite sills have been dated at 730 Ma, making them the youngest igneous rocks in the area (Channer *et al.* 1998).

Crystals of diamond were found in all the sills. Some of their characteristics were described in previous studies (Svisero & Baptista 1973, Nixon *et al*. 1992, Meyer & McCallum 1993), but there has been no systematic study to date.

The main objectives of this work were as follows: 1) to conduct the first comprehensive mineralogical study of diamond from Guaniamo in order to identify characteristic features, 2) to evaluate the conditions of formation of the diamond, and 3) to identify the primary sources for the placer deposits in both the Quebrada Grande Valley and nearby alluvial areas.

For this purpose, we have studied more than 5,000 crystals of diamond from several kimberlite sills (Los Indios – 024, Candado, and Bicicleta) and placer deposits (Quebrada Grande, Ringi–Ringi, Chihuahua and La Centella). The locations of these deposits areas are shown in Figure 2, except for La Centella, which lies *ca*. 8 km northeast of Milagro town, in the valley of the Cuchiverito River, outside the Quebrada Grande basin.

TABLE 1. GRAIN-SIZE DISTRIBUTION OF THE DIAMOND SAMPLES, GUANIAMO AREA, VENEZUELA

Location	Number of diamond crystals or fragments	Mass cts	–4 +2 mm % total number	–4 +2 mm % total mass	–2 +1 mm % total number	–2 +1 mm % total mass	–1 +0.5 mm % total number	–1 +0.5 mm % total mass
Kimberlite sills								
Los Indios	43	0.98	7.0	27.8	41.8	51.9	51.2	20.3
Area 024	1434	46.28	6.2	30.2	69.5	60.6	24.3	9.2
Candado	25	0.62	4.0	11.4	60.0	69.4	36.0	19.2
Bicicleta	76	2.30	6.6	23.8	68.4	65.7	25.0	10.5
Kimberlite sills total	1578	50.18	6.2	29.7	68.6	60.7	25.2	9.6
Placer deposits								
Quebrada Grande	1990	75.83	9.4	39.6	59.4	52.2	31.2	8.2
Ringi–Ringi	144	30.32	100.0	100.0	0.0	0.0	0.0	0.0
Chihuahua	130	30.96	73.1	90.6	26.9	9.4	0.0	0.0
La Centella	201	11.55	23.5	41.9	76.5	58.1	0.0	0.0

INFORMATION ABOUT SAMPLES

Diamond crystals from the kimberlite sills were obtained from sampling programs run by the Guaniamo Mining Company. Samples from the Quebrada Grande and La Centella placers were purchased from local miners, and those from the Ringi–Ringi and Chihuahua placers were supplied from the company's collections. Information regarding numbers and size distributions of the diamond samples is given in Table 1.

Note that the quantities of diamond from individual kimberlite sills are relatively small. Most of the diamond crystals are small, with 25% in the range –1 +0.5 mm, 69% in the range –2 +1 mm, and only 6% in the range –4 +2 mm (Table 1). The majority of the diamond crystals from the Quebrada Grande placer fall within the –2 +1 mm range (59%) and –1 +0.5 mm range (31%). The sample from La Centella only contained diamond crystals in the –4 +2 mm (23.5%) and –2 +1 mm (76.5%) ranges. The samples from Ringi–Ringi and Chihuahua are dominated by the coarser –4 +2 mm fraction (100% and 73%, respectively) and do not contain –1 +0.5 mm diamond (Table 1).

ANALYTICAL METHODS

Analytical work included characterization of diamond morphology and color, ultraviolet luminescence, infrared spectroscopy, carbon isotopic composition, and the identification and analysis of mineral inclusions. All analytical work was performed in Moscow apart from trace-element analysis of diamond inclusions, which was done at Macquarie University.

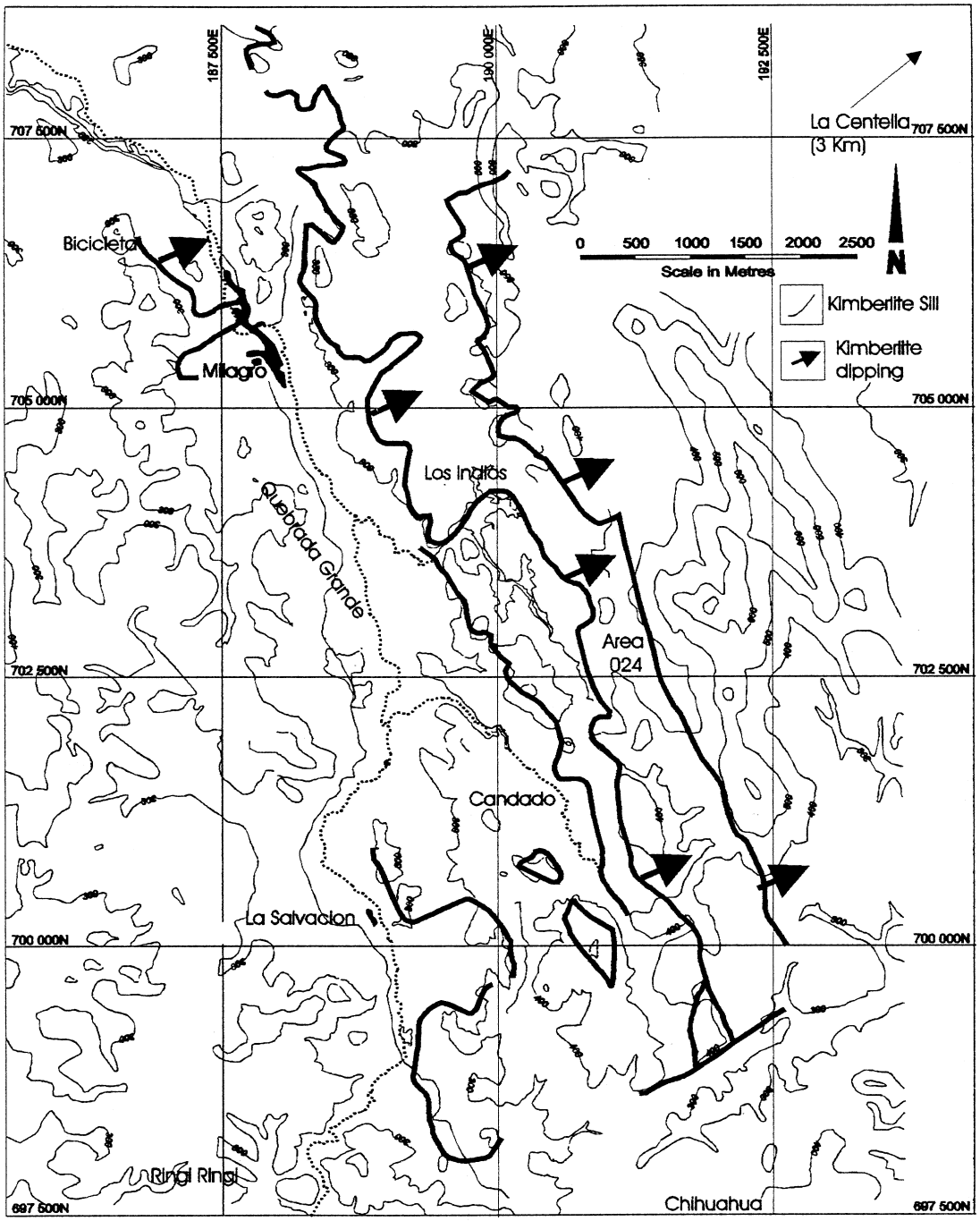

FIG. 2. Locations of sample sites in Guaniamo. Contours are 100 m, major watercourses indicated by dotted lines.

TABLE 2. MORPHOLOGY OF DIAMOND FROM THE GUANIAMO AREA

Location	Number of diamond crystals	Octahedra	Dodeca-hedra	Combi-nation of types	Uncer-tain types
		Kimberlite sills			
Los Indios	30	0.0%	46.4%	25.0%	28.6%
Area 024	1203	2.4	48.9	14.9	33.8
Candado	23	5.5	55.6	33.4	5.5
Bicicleta	55	0.0	55.5	18.5	26.0
Kimberlite sills total	1311	2.1	49.7	16.3	31.9
		Placer deposits			
Quebrada Grande	794	5.1	44.5	10.1	40.3
Ringi–Ringi	144	9.0	46.6	32.6	11.8
Chihuahua	130	6.9	44.6	35.4	13.1
La Centella	201	5.5	49.2	23.4	21.9

The ultraviolet (UV)-induced luminescence of diamond samples was studied with a "Lusam-R" apparatus. Photoluminescence (PL) was induced by a SVD–120A mercury–quartz lamp with an UFS–6 filter.

Infrared (IR) spectra were obtained at the Institute of Diamonds in Moscow, using a Specord M–80 spectrometer (Karl Zeiss, Jena) with a beam condenser. Spectral resolution was 6–10 cm^{-1}. Concentrations of A and B nitrogen centers were calculated according to the IR absorption coefficients specified by Boyd *et al*. (1994, 1995). For mixed IaAB type of diamond, the Mendelssohn & Milledge (1995) method was used. Errors on the determined concentrations are less than 25%.

Isotope analyses were performed by K. Maltsev, GEOHI, with the VARIAN–MAT 230 mass spectrometer, with an accuracy of <0.1‰ PDB ($^{13}C/^{12}C$ PDB = 0.0112372). After initial preparation, crystals of diamond were oxidized to CO_2 using an O_2 flux (circular system, 900°C).

Inclusions were extracted from their hosts by cracking, and analyses of these for major and minor elements were carried out using a Camebax electron microprobe, with an acceleration voltage of 15 kV and a beam current of 15 mA.

The concentrations of selected trace elements were acquired using a laser-ablation microprobe – inductively coupled plasma – mass spectrometer (LAM–ICP–MS) at the School of Earth Sciences, Macquarie University, following procedures outlined by Norman *et al*. (1996, 1998). Glass NIST610 was used as the external standard, and Ca as the internal standard. Because most of the analyzed inclusions were very small, very low laser energies were required, which resulted in low signals and significantly higher detection-limits than are normally achieved (*cf*. Norman *et al*. 1998).

Morphology of the Diamond Crystals

Diamond crystals from the Guaniamo area include octahedral, dodecahedral, O–D combination-type and cubic crystals, and their twins and aggregates. There is also a rather high proportion of grains of uncertain morphology (typically with spalled surfaces) and unclassifiable habit.

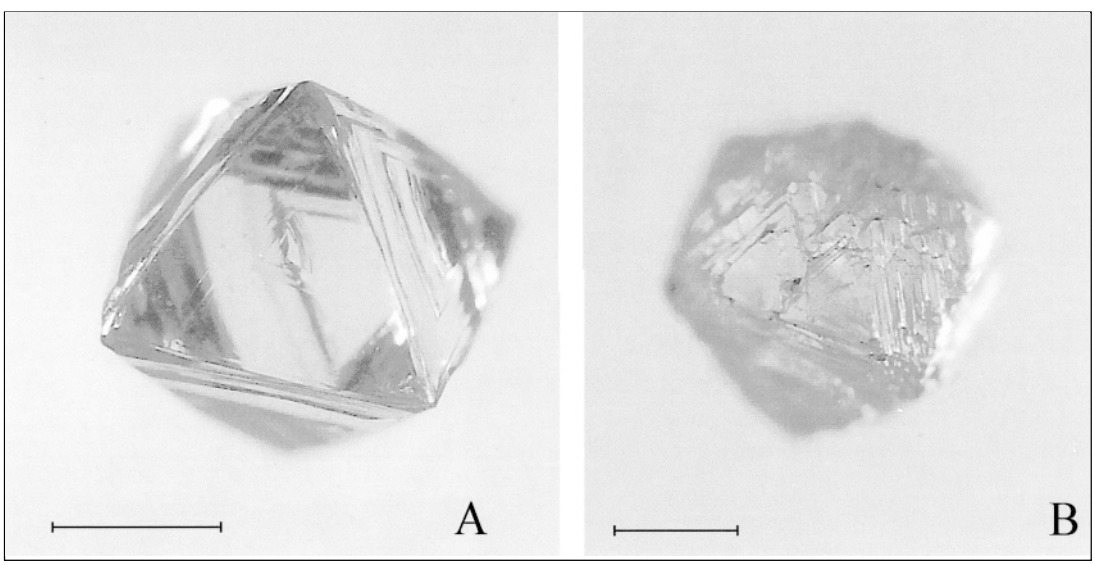

FIG. 3. Surface textures of octahedra of diamond. A) Stepwise lamellar development of trigonal faces. B) Polycentric development of crystal faces. Scale bar is 1 mm.

In all the sills and placer deposits studied, rhombicododecahedral crystals are predominant, accounting for about 50% of the samples (Table 2). Combination-type O–D crystals also are present in rather high proportions, especially in the La Centella placer, where they account for 23.4% of the total. The proportion of octahedra among sill-hosted diamond crystals is about 2%, compared with that of placer-hosted diamond crystals, which reaches as high as 5%. As shown in Table 2, each sill exhibits different proportions of the main morphological types of diamond.

Octahedral diamond with flat faces and sharp edges is rare. More commonly, the crystals have two types of growth features: (1) stepwise lamellar development of trigonal faces (Fig. 3A), with different thickness of growth layers, and (2) polycentric development of crystal faces. During growth of the faces of these latter crystals, plates tend to develop from several centers, giving their surfaces a distinctive appearance (Fig. 3B).

The rhombicododecahedral habit of diamond is a resorption-induced form. Among man-made crystals of diamond, dodecahedra formed as a result of growth processes have never been found. Dodecahedral crystals of diamond are usually called "dodecahedroids" because of their roundish shape. In some articles, they were called "tetrahexahedroids" (*e.g.*, Robinson *et al.* 1989). This is an obvious misunderstanding because in contrast to a dodecahedron with twelve rhombic faces, a tetrahexahedron is a variety of a cubic shape with twenty-four trigonal faces (see below).

Dodecahedral crystals of diamond from Guaniamo are represented by a wide variety of rounded, dodecahedroidal shapes, from perfect crystals to strongly distorted, irregularly shaped ones. They are subdivided into the following three groups on the basis of the nature of the distortion.

1) Isometric, non-distorted crystals are regular rhombicodecahedroids with rhombic convex faces separated by rectilinear face sutures along the short diagonal of the rhomb into two symmetrical spherical triangles. The majority of isometric dodecahedroids exhibit very little divergence from the ideal shape.

2) Dodecahedroids flattened along the [111] axis commonly form spinel-type twins. The degree of flattening in this direction varies from negligible to sufficient to result in pseudoditrigonal crystals.

3) Dodecahedroids featuring complicated distortion, *i.e.,* distorted along several crystallographic directions, commonly exhibit specific peculiar shapes with unevenly developed faces forming irregular polygons. Other types of distortion occur more rarely.

Dodecahedroids with completely smooth surfaces are observed in very rare cases. Most commonly, crystal faces exhibit a variety of accessory and surface features of different forms and sizes, which are the results of plastic deformation of the diamond crystals and surface dissolution by oxidation reaction.

A distinctive feature of diamond crystals from all the areas studied is the presence of bands of plastic deformation. Plastic deformation is recorded on crystal surfaces by the emergence of gliding dislocations, resulting in distinct striations or thick banding. Dissolution of the diamond produces shagreen, hackly [with hillocks: Robinson *et al.* (1989); Fig. 4A], droplet (Fig. 4B), grooved (with wide hillocks, Fig. 4C) and block-type features. In some cases, the dissolution exhibits initial octahedral growth-steps (Fig. 4D).

The O–D (octahedron + dodecahedroid) combination-type diamond has almost evenly developed (111) and (110) faces.

Single *cubic-habit crystals* were found only in the Guaniamo placer. They are represented by tetrahexahedroids (rounded tetrahedral form) and combination-type crystals. Tetrahexahedroid crystals are equant, grey, and non-transparent. They contain numerous inclusions of graphite and exhibit shagreen surfaces.

Combination-type diamond of cubic habit typically consists of equant brown crystals representing a combination of cubic, octahedral, and dodecahedroidal habits. The (100) cubic surfaces are flat, with tetragonal pitting. Crystal apices are blunted by flat (111) octahedral faces, and (110) surfaces covered with step-like or columnar features are developed at crystal edges.

Crystals of different habit form *twins and aggregates*. Twins are predominantly trigonal (in plan view) macles formed by octahedra. Dodecahedroid twins look like spherical trigons in plan view. In rare cases, there are dodecahedroid penetration twins (Fig. 5A) or their complex twin intergrowths.

Aggregates typically form comparatively large crystals. They may consist of intergrowths of smaller crystals into larger ones, or parallel, irregular (Fig. 5B), or polycrystalline growths. Twins themselves also form spinel-type and complex twin intergrowths and aggregates.

Many of the diamond crystals or fragments studied show evidence of *natural oxidative dissolution*, in the form of etch channels and patterns, vugs, and corroded surfaces. Among the accessories produced by oxidative dissolution *on the faces of octahedra*, inversely parallel trigonal pit-like etch patterns are the most abundant. In cases where angles are blunted, these pits occur on tetra-, penta- and hexagonal shapes. In some cases, they occur as isolated pits, in other cases in groups, and may form a continuous pattern on (111) faces. The pits show a variable degree of coarseness, from gentle ones visible only at high magnifications, to coarse ones. In some cases, triangular pits are overprinted by smaller second-generation ones.

In addition to the surface features described above, natural dissolution of *dodecahedroid crystals* results in the formation of etch channels (Fig. 6) and vugs, the walls and bottoms of which are commonly characterized by step-like surfaces. Small etch triangles are also typically present along with striations.

Typical *erosion marks* on diamond are glossy spalled surfaces with sharp edges developed to different degrees, from very fine pits on the edges of intact crystals to acute-angular fragments spalled on all sides. These spalled surfaces, much like the surfaces of spalled crystals, typically show no direct evidence of abrasion other than fractured and crumpled thin, sharp edges. In rare cases, crystals with single surficial fissures oriented perpendicular to crystal edges were found. In more than 99% of the diamond crystals studied, no crescentiform and annular fissures, rhombic pattern, or abrasion dulling on the faces, blunting and rounding of edges and apices, were observed. However, our diamond collection from the Quebrada Grande placer does contain single crystals that show evidence of intensive abrasion. The faces of these crystals show numerous small crescentiform fissures, and their edges and apices are slightly spalled.

Diamond Color and Transparency

The majority of the diamond crystals from the Guaniamo region are colorless; colored stones are smoky-brown, grey and green (Table 3). The smoky-

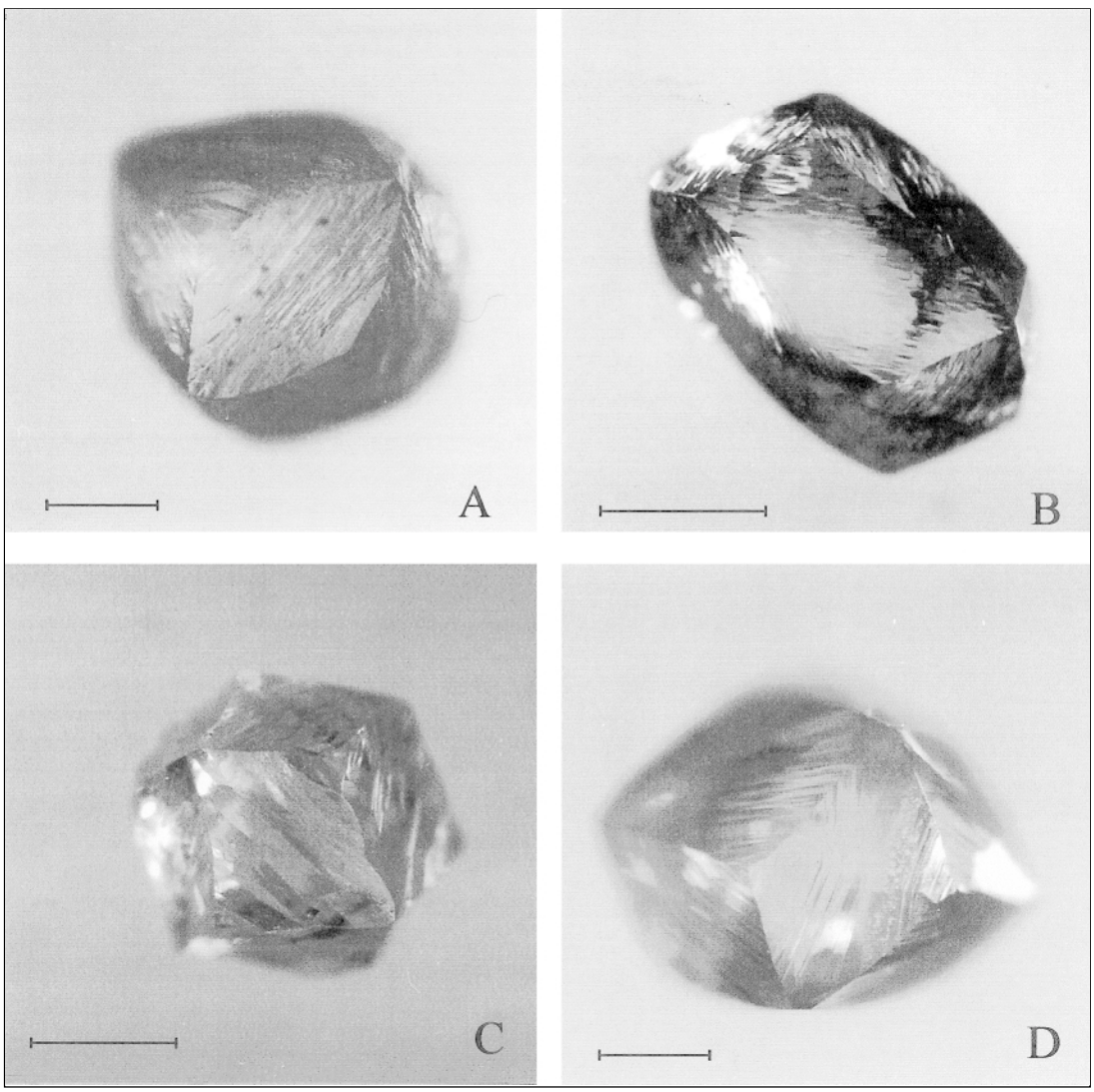

FIG. 4. Surface textures of rhombicododecahedral diamond. A) Hackly surface. B) Droplet surface. C) Grooved surface. D) Octahedral growth-steps exposed by dissolution. Scale bar is 1 mm.

brown color results from plastic deformation, whereas the grey color is caused by the presence of numerous black graphite-like inclusions (Orlov 1987). In addition to green-colored diamond, there is also green-spotted diamond; 55–90% of the crystals show isolated bright green spots on their surface (Fig. 4A). They are developed on diamond crystals of all colors. Several cases of diamond with brown spots were found in the Quebrada Grande placer collection as well. Some crystals show a rusty or black color, due to the occurrence of iron hydroxides or black host-rock material in joints, etch channels, and surficial pits. Such diamond is especially common among the +2 mm crystals.

Diamond crystals from the kimberlite sills and the Quebrada Grande placer have similar color distributions, whereas the La Centella placer contains a higher proportion of green diamond and fewer colorless and grey diamond (Table 3). The Ringi–Ringi and Chihuahua placers have much lower proportions of grey stones, and much higher proportions of green diamond, than the Quebrada Grande placer. They also contain yellow diamond, which is absent in the Quebrada Grande placer. In the Quebrada Grande placer, smaller size-fractions have higher proportions of smoky brown and green stones. In the Chihuahua placer, the smaller diamond crystals (–2 +1 mm fraction) show a higher proportion of green diamond but no yellow stones.

Diamond crystals from the kimberlite sills and the Quebrada Grande and La Centella placers are more than 50% semitransparent, and less than 20% are very transparent or transparent. In contrast, the Ringi–Ringi and Chihuahua placers both contain more than 65% very transparent or transparent stones.

Diamond Photoluminescence

All diamond crystals studied were subdivided into two groups based on the distribution of photoluminescence (PL) color: homogeneous and heterogeneous. Diamond crystals with heterogeneous PL, which are uncommon, were subdivided into zoned and block-type crystals. These features demonstrate the layer-by-layer and block-type growth of diamond crystals.

Most of the samples show a blue PL color, and a relatively high proportion of crystals exhibit no visible luminescence (Table 4). Yellow PL is the next most common, whereas green and pink colors occur rarely.

TABLE 3. COLORATION OF DIAMOND AT GUANIAMO

Location	Number of diamond samples	Color-less	Smoky brown	Grey	Green	Yellow	Total	With pig-ment spots
Kimberlite sills								
Los Indios	30	53.5%	17.9%	0.0%	28.6%	0.0%	100.0%	57.1%
Area 024	1203	55.8	11.4	21.6	11.2	0.0	100.0	54.1
Candado	23	11.1	55.6	22.2	11.1	0.0	100.0	77.8
Bicicleta	55	27.8	25.9	24.1	22.2	0.0	100.0	75.9
Kimberlite sills total	1311	51.7	14.5	20.7	13.1	0.0	100.0	57.1
Placer deposits								
Quebrada Grande	794	49.0	19.7	19.2	12.1	0.0	100.0	69.5
Ringi - Ringi	144	69.4	6.2	2.1	17.4	4.9	100.0	81.9
Chihuahua	130	40.0	18.5	6.9	33.1	1.5	100.0	88.5
La Centella	201	40.8	22.9	9.4	26.9	0.0	100.0	79.1

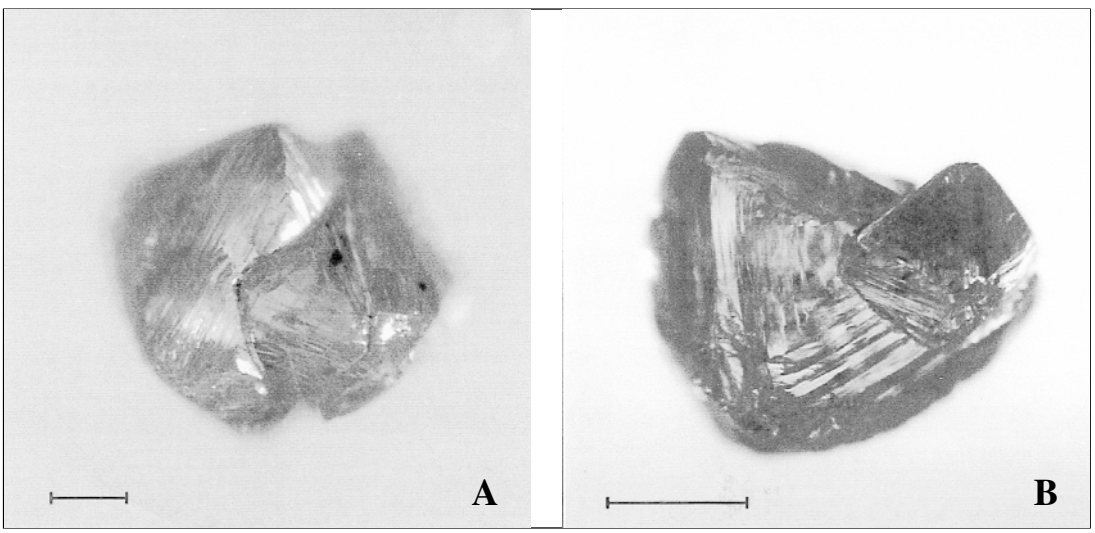

FIG. 5. Morphologies of twinned and aggregate diamond. A) Dodecahedroid penetration twin. B) Aggregate of combination-type crystals of unequal size. Scale bar is 1 mm.

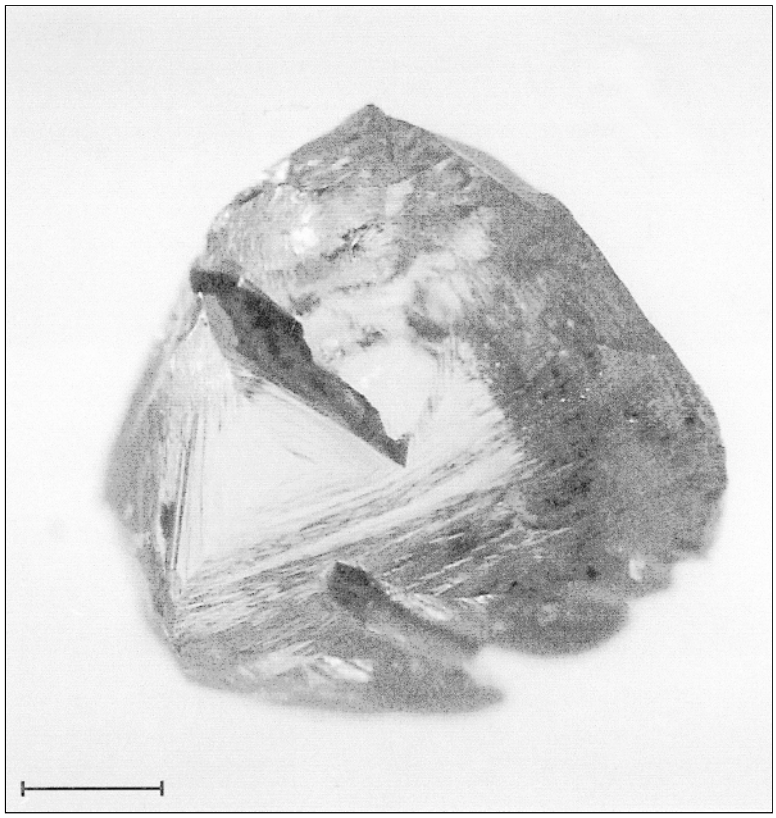

FIG. 6. Combination-type O–D crystal with etch channels. Scale bar is 1 mm.

In general, the PL characteristics of diamond crystals from the Guaniamo sills are identical to those of diamond from the Guaniamo placer deposit. Of the crystals in these two groups, 55.8% and 58.6%, respectively, have a blue luminescence (Table 4). The other PL properties also are similar in these deposits. Hence, diamond crystals from the sills and the Quebrada Grande placer are essentially identical in their luminescence properties. The La Centella, Ringi–Ringi and Chihuahua placers have higher proportions of diamond crystals with blue PL (>75%) and lower proportions of diamond crystals with no PL than the sills and the Quebrada Grande placer. This finding is consistent with other specific features of the La Centella, Ringi–Ringi and Chihuahua populations of diamond, which contrast to the other populations.

Infrared Spectroscopy and Nitrogen Impurities

Structural impurities in natural diamond reflect the conditions of formation and mantle residence of diamond and may be used as a "fingerprinting" tool (Kaminsky *et al.* 1988). More than twenty types of nitrogen impurities occur in diamond, as well as hydrogen and boron impurities (Scarratt 1992). In this work, we used infrared (IR) spectroscopy to estimate the concentrations of two major types of nitrogen impurity, A and B.

IR spectra of diamond grains from the sills and placer deposits are rather similar. They all show bands representing A and B nitrogen impurities and do not show resolvable concentrations of single nitrogen-atom impurities of type Ib. Grains of type-II (nitrogen-free) diamond were not found in the samples studied. All Guaniamo diamond samples studied belong to the transitional IaAB type. As many as 20% of all diamond grains studied contain low (<250 ppm) concentrations of all nitrogen impurities.

The majority of the diamond crystals or fragments studied show a predominance of B-type nitrogen impurities, although in a few crystals, A-type nitrogen impurities are more abundant.

Concentrations of A-type nitrogen impurities range from 19 to 548 ppm (average 195 ppm; Table 5). B-

TABLE 4. PHOTOLUMINESCENCE OF DIAMOND AT GUANIAMO

Location	Number of diamond crystals or fragments	Homogeneous					Heterogeneous		
		Blue	Yellow	Green	Pink	Uncert.	Non-Fluor.	Zoned	Block-Type
Kimberlite sills									
Los Indios	30	66.7%	6.7%	3.3%	0.0%	0.0%	20.0%	3.3%	0.0%
Area 024	1203	55.8	8.7	2.8	1.7	6.3	14.2	6.3	4.2
Candado	23	50.0	16.7	0.0	0.0	0.0	22.2	11.1	0.0
Bicicleta	55	47.8	21.7	0.0	10.9	0.0	19.6	0.0	0.0
Kimberlite sills total	1311	55.8	9.2	2.7	1.9	5.8	14.7	6.1	3.9
Placer deposits									
Quebrada Grande	794	58.6	8.6	1.5	3.2	11.7	13.0	1.7	1.7
Ringi - Ringi	144	85.4	2.8	0.7	0.7	2.1	2.1	3.4	2.8
Chihuahua	130	83.0	0.8	0.0	0.0	2.3	11.5	1.6	0.8
La Centella	201	77.1	8.9	1.5	1.5	0.0	6.5	4.5	0.0

type nitrogen impurities have concentrations ranging from 27 to 1256 ppm (average 438 ppm). The aggregation coefficient, 100 B/(A + B), is rather high, averaging *ca*. 70% for all the Guaniamo diamond samples. Diamond samples from the kimberlite sills and the Quebrada Grande placer have similar aggregation coefficients (70.1% and 71.0%, respectively), whereas these values are lower in the diamond from Ringi–Ringi and Chihuahua (66.8% and 65.3%, respectively).

Figure 7 shows the structural impurity data for the diamond samples plotted against the number of crystals. The B-center distribution is of particular interest. In general, the diamond samples from the kimberlite sills and the Quebrada Grande placer deposits show a coincidence of the positions of major peaks, consistent with a kimberlite-sill source for most of the placer diamond. An additional peak in curve 2 suggests an additional source of diamond in the Quebrada Grande placers, distinct from the known sills. The diamond grains from the other placer deposits (La Centella, Ringi–Ringi and Chihuahua) are clearly distinct from the diamond grains of the known kimberlite sills in terms of their B-center distribution.

TABLE 5. GENERAL CHARACTERISTICS OF NITROGEN CENTERS IN DIAMOND AT GUANIAMO

Location	Number of diamond samples	Average, at. ppm		Aggregation
		A	B	
Kimberlite sills				
Total	49	181	425	70.13%
Placer deposits				
Quebrada Grande	40	205	502	71.00
Ringi–Ringi	33	215	433	66.82
Chihuahua	31	223	420	65.32
La Centella	39	162	409	71.63
Average	192	195	438	69.19

Carbon Isotopic Composition of Diamond

In total, 108 samples were analyzed, 48 of which are from the sills (Table 6). For most of these stones, the paragenesis was defined by mineral inclusions (see below). The total range in the isotopic composition $\delta^{13}C$ of the analyzed crystals is from –3.2‰ to –28.7‰. There seems to be no correlation between diamond morphology and carbon isotopic composition.

A $\delta^{13}C$ histogram (Fig. 8) shows a small peak between –3‰ and –9‰, which is dominated by diamond of the peridotitic paragenesis. This peak corresponds closely to the worldwide mean for diamond of the peridotitic paragenesis, with the mode close to the "mantle value" of –4.5 to –5.0‰ (*e.g.*, Galimov 1968, Deines 1992). The major peak from –10‰ to –20‰ is composed entirely of diamond of the eclogitic paragenesis, and in some cases, diamond from this paragenesis contains even lighter carbon (to $\delta^{13}C$ = –28.7‰). To our knowledge, isotopically light diamond is the predominant type only in four localities: (1) Argyle pipe, Australia (Sobolev *et al*. 1989), (2) Sloan pipe in the Wyoming–Colorado area, U.S.A. (Otter *et al*. 1989), (3) Dachine ultramafic rocks in French Guiana (McCandless *et al*. 1999), and (4) Ebelyakh placer, northern Siberia, of unknown affiliation (Galimov *et al*. 1978). In all other diamondiferous regions, including the main kimberlite pipes of South Africa and Siberia, isotopically heavy diamond predominates, comprising up to 99% of all diamond samples analyzed.

Galimov *et al*. (1999) presented isotopic data for 63 diamond samples from Guaniamo placers and two sills. Values of $\delta^{13}C$ ranges from –8‰ to –26.5‰, within the range of the data presented in this study. Thirty-one of the diamond samples analyzed by Galimov *et al*. (1999) contained inclusions. Of these, 30 were of the eclogitic paragenesis. The smaller peak centered at $\delta^{13}C$ = –6‰ was not observed by Galimov *et al*. (1999), probably because of the near-absence of diamond of the peridotite paragenesis in their sample. The one diamond with a peridotitic inclusion (chromian spinel) has $\delta^{13}C$ = –8.3‰, within the range of data reported here.

The correlation between carbon isotope composition and mineral paragenesis in the Guaniamo data reported here and by Galimov *et al*. (1999) is good enough to allow a paragenesis to be assigned to diamond grains lacking inclusions, with a high degree of confidence. On the basis of these 200 analyses, we estimate that 93 ± 2% of the Guaniamo diamond population is derived from eclogitic host-rocks.

Mineral Inclusions in Diamond

Syngenetic mineral inclusions in natural diamond worldwide fall into three main paragenetic suites: the peridotitic suite (UM or P type), the eclogitic suite (E type) and the superdeep suite (SD type), representing diamond derived from the lower mantle and transition zone. These three paragenetic suites correspond to distinct environments of diamond growth (Meyer 1982, Harte & Harris 1994, Davies *et al*. 1999). Diamond grains from the Guaniamo district contain mineral inclusions of all three suites.

Ninety-three inclusions were extracted from 77 grains of diamond, of which ten (13%) are of the peridotitic paragenesis and one is of the superdeep paragenesis (Table 7). The remaining 85.7% are diamond grains of the eclogitic paragenesis.

The eclogitic paragnesis

In the Guaniamo suite, inclusions of the *eclogitic paragenesis* (E type) consist of garnet, clinopyroxene, rutile, ilmenite, pyrrhotite, and probable coesite. This association was described in general terms by Sobolev *et al.* (1998).

Garnet of the pyrope–almandine series is the most abundant E-type inclusion. Thirty-seven inclusions of garnet from 11 diamond grains from the four sills, 16 diamond grains from the Quebrada Grande placer, and 9 diamond grains from the La Centella placer were analyzed (Table 8). Most of these (74%) have high Ca contents (>8% CaO). This feature was previously observed in garnet inclusions in diamond from the Argyle pipe, Australia (Jaques *et al*. 1989, Sobolev *et al*. 1989) and from a number of pipes of the Arkhangelsk region (Zakharchenko *et al.* 1991). Most of these garnet inclusions have Na contents similar to those of garnet from diamondiferous eclogites (McCandless & Gurney 1989), but lower than those of many examples of garnet of eclogitic affinity included in diamond from the Argyle lamproite (Jaques *et al*. 1989, Sobolev *et al*. 1989).

Figure 9 shows the Mg–Ca–Fe proportions of the garnet inclusions (including Cr-rich varieties; see below). The compositions of garnet inclusions from the sills and placer deposits of the Guaniamo area define a compact field similar to that of garnet from kyanite- and corundum-bearing eclogites. These garnet grains have simple rare-earth element (*REE*) patterns, characterized by enrichment in the heavy rare-earth elements (*HREE*) and moderate depletion in the light rare-earth elements

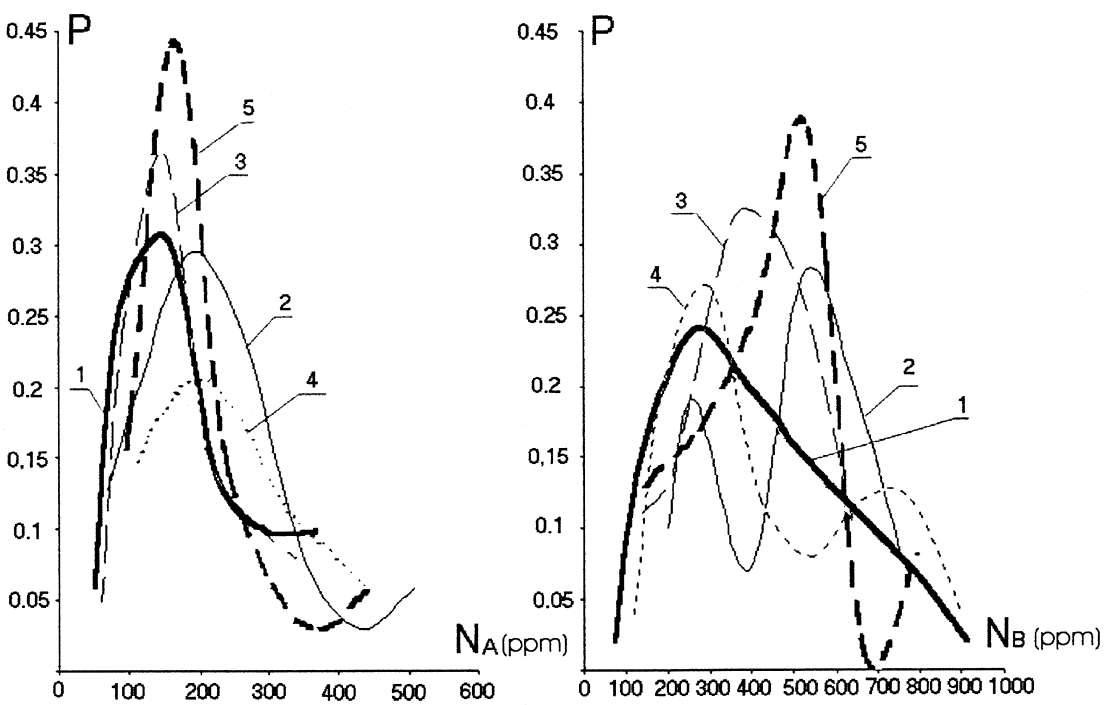

FIG. 7. Frequency (P) of nitrogen-impurity abundance (in ppm). Graphs for A and B impurity types are shown for the Guaniamo sills (1), the Quebrada Grande placer (2), the La Centella placer (3), the Ringi–Ringi (4) and Chihuahua (5) placers.

TABLE 6. CARBON ISOTOPIC COMPOSITION OF DIAMOND AT GUANIAMO

Sills

Sample	Morphology	Type	$\delta^{13}C$ PDB
Los Indios			
001	O+D combination	E	-14.7‰
001a	Dodecahedroid	E*	-17.1
Area 024/1			
014	O+D combination	E	-21.2
017	Dodecahedroid		-15.8
019	O+D combination	E	-15.4
021	O+D combination		-10.1
024	Dodecahedroid	E	-11.6
029	Twin of combination-type O+D		-16.4
035a	Dodecahedroid		-16.4
035b	Twin of combination-type O+D		-18.6
035c	Dodecahedroid		-18.3
037a	Twin of combination-type O+D	E	-18.6
037b	Dodecahedroid	E*	-15.2
037c	Dodecahedroid	E	-16.8
037d	Dodecahedroid	E*	-15.2
040	Twin of combination-type O+D	P	-5.4
043	Dodecahedroid	E	-17.7
047	O+D combination		-18.5
051a	O+D combination	E	-19.1
051b	Dodecahedroid	E	-20.7
052	Dodecahedroid	E	-16.3
053	Dodecahedroid	E	-16.9
053a	O+D combination	E*	-12.5
054	O+D combination		-14.7
055	Twin of dodecahedroids	E	-13.4
056	O+D combination	E	-6.9
057	O+D combination		-10.2
060	Dodecahedroid	E	-12.8
063a	Dodecahedroid	E	-16.7
063b	Dodecahedroid	E	-18.3
064a	Dodecahedroid	E	-14.4
064b	Dodecahedroid	E*	-11.5
Area 024/3			
003	O+D combination		-15.9
010a	Twin of combination-type O+D	E	-12.9
010b	Twin of combination-type O+D	E*	-25.0
010c	Dodecahedroid	E*	-11.9
010d	Dodecahedroid	E*	-17.2
011a	Twin of dodecahedroids	E*	-19.9
011b	O+D combination	E*	-16.1
012	Dodecahedroid	E	-10.4
012a	Dodecahedroid	E	-15.1
013	Dodecahedroid	E	-11.7
Candado Julio			
006a	O+D combination	E	-15.5
006b	Dodecahedroid	E*	-17.8
006c	Dodecahedroid	E*	-24.8
008	Twin of combination-type O+D		-13.0
Bicicleta			
004	Dodecahedroid	E	-17.6
005	Twin of combination-type O+D		-16.5

Placer deposits

Sample	Morphology	Type	$\delta^{13}C$ PDB
Quebrada Grande			
V-1	Twin of dodecahedroids	P	-8.4‰
V-2	Twin of dodecahedroids	P	-3.2
V-3	Twin of dodecahedroids		-14.7
V-5	O+D combination	P	-6.2
V-6	Dodecahedroid	E	-13.7
V-7	O+D combination	E	-14.4
V-8	Octahedron	E	-12.3
V-9	Dodecahedroid	E	-15.2
V-11	Dodecahedroid	E	-14.5
V-14	O+D combination	E	-14.9
V-15	Dodecahedroid	E	-11.8
V-17	O+D combination	E	-12.6
V-19	O+D combination	E	-18.2
V-20	Dodecahedroid	E	-17.0
V-21	Dodecahedroid	E	-10.1
V-22	Octahedron	E	-13.6
V-23	Dodecahedroid	E	-14.4
V-24	Dodecahedroid	E	-12.7
V-25	Dodecahedroid	E	-15.3
V-26	O+D combination	E	-9.5
V-27	Dodecahedroid	E	-22.0
V-28	Dodecahedroid	P	-7.3
V-29	Dodecahedroid	E	-17.9
V-30	Dodecahedroid	E	-12.8
V-31	Dodecahedroid		-14.4
V-32	Twin of dodecahedroids	E	-16.7
V-33	Dodecahedroid	E	-17.1
V-34	Dodecahedroid		-3.4
V-35	Cube		-10.1
V-36	Twin of dodecahedroids	P	-4.9
La Centella			
1442	Dodecahedroid		-13.2
1448	O+D combination	E	-24.6
1449	Dodecahedroid		-10.9
1450	Dodecahedroid		-11.8
1451	O+D combination	E	-17.3
1453	Twin of combination-type O+D		-22.5
1509	Dodecahedroid		-20.5
1810	Dodecahedroid	E	-14.9
1812	Dodecahedroid	P	-6.8
1813	O+D combination		-25.2
1815	Dodecahedroid	E	-15.9
1871	Dodecahedroid		-12.3
1877	Octahedron	E	-12.2
1943	Dodecahedroid		-14.8
1946	Dodecahedroid		-11.1
1969	Dodecahedroid		-15.1
1989	Twin of dodecahedroids		-15.2
1991	Twin of dodecahedroids	E	-16.4
2086	Dodecahedroid		-14.8
2089	Twin of dodecahedroids	E	-28.7
2100	O+D combination		-13.4
2127	Dodecahedroid	E	-13.9
2135	O+D combination		-12.9
2138	Dodecahedroid	E	-20.9
2208	Dodecahedroid	E	-23.1
2212	Dodecahedroid	E	-23.3
2214	Dodecahedroid	E	-12.3
2215	O+D combination		-16.9
2217	O+D combination	E	-12.7
2220	Dodecahedroid	E	-17.9

Symbols: E: eclogitic paragenesis, P: peridotitic paragenesis. * Inclusions not analyzed.

TABLE 7. MINERALS AND MINERAL ASSOCIATIONS INCLUDED IN DIAMOND AT GUANIAMO

Sills

	Eclogitic Paragen.						Perid. Paragen.			SD
	G	C	R	I	S	In	P	O	Ch	Pe
Los Indios										
001*		1								
Candado Julio										
006a*	1									
Area 024/1										
014*	1§									
018		1§								
019*		1§								
024*	1									
037a*	1									
037c*		1								
039				1						
040*								2§		
043*	1									
051a*	1									
051b*	1									
052*	1									
053*	1									
055*			1							
056*					1					
060*		1								
063a*		1§								
063b*		1§								
064a*		1								
Area 024/3										
010a*		1								
012*	1	1§				GC				
012a*		1§								
013*		1								
Bicicleta										
004*	1									

Placer deposits

	Eclogitic Paragen.						Perid. Paragen.			SD
	G	C	R	I	S	In	P	O	Ch	Pe
Quebrada Grande										
V-1*							1§			
V-2*							1§			
V-4									1	
V-5*								2		
V-6*	1									
V-7*	1									
V-8*		1								
V-9*	1									
V-11*		1								
V-12	1				2	GS				
V-13									1	
V-14*	1									
V-15*				2						
V-16	1									
V-17*		2								
V-18	2									
V-19*	1	1				GC				
V-20*		1								
V-21*		2								
V-22*		1								
V-23*		1								
V-24*	1									
V-25*	1	1				GC				
V-26*	2									
V-27*	1									
V-28*								1		
V-29*		1								
V-30*	1									
V-32*	1									
V-33*				1						
V-36*							2			
V-37		1								
V-38									1	
V-40										1
La Centella										
1448*	1§	1				GC				
1451*		1								
1504	1§	1				GC				
1518		1								
1810*	1									
1812*									1	
1815*		1§								
1877*	1§	1				GC				
1991*	1§									
2089*		1								
2127*		1								
2138*	1									
2208*		1								
2212*	1									
2214*	1§									
2217*		1								
2220*	1									
Total	36	34	2	4		7	4	5	4	1

Column headings: defining the eclogitic paragenesis, G: garnet, C: clinopyoxene, R: rutile, I: ilmenite, S: sulfides, In: intergrowth; defining the peridotitic paragenesis, P: pyrope, O: olivine, Ch: chromian spinel; considered diagnostic of a Superdeep assemblage (SD), Pe: ferroan periclase. In the column describing intergrowths, GC: garnet + clinopyroxene, GS: garnet + sulfide. * Diamond sample analyzed for $\delta^{13}C$. § Mineral grains analyzed for trace elements with LAM–ICP–MS.

(*LREE*) (Table 9, Fig. 10A). Their Y contents are similar to those of Argyle garnet inclusions, but their Zr contents are significantly lower (Fig. 11A). Their Y/Zr values are similar to those of garnet from many diamondiferous eclogites. Their Sr contents are intermediate between the high values found in inclusions from the Argyle suite of diamond and the low values found in the garnet of many eclogite xenoliths, both diamondiferous and barren (Griffin *et al*. 1988; Fig. 11B).

TABLE 8. COMPOSITION OF GARNET INCLUDED IN DIAMOND AT GUANIAMO

Sample	SiO_2	TiO_2	Al_2O_3	Cr_2O_3	FeO	MnO	MgO	CaO	Na_2O	Total
Area 024/1 sill, almandine–pyrope, eclogitic paragenesis										
014*	39.89	0.64	21.82	0.07	16.05	0.26	9.85	10.72	0.25	99.55
024	39.66	0.52	22.01	0.02	18.16	0.42	9.21	8.79	0.15	98.94
037a	39.21	0.69	21.63	0.02	15.61	0.39	7.85	13.30	0.21	98.91
043	39.10	0.57	21.68	0.03	17.71	0.31	10.36	8.57	0.21	98.54
051a	39.76	0.61	21.68	0.02	16.88	0.32	10.77	8.59	0.14	98.77
051b	39.68	0.48	21.64	0.09	17.27	0.47	9.35	10.31	0	99.29
052	39.19	0.61	21.64	0.08	17.47	0.31	10.88	8.65	0.22	99.05
053	39.98	0.46	21.33	0.05	16.02	0.31	8.46	12.10	0.26	98.97
Area 024/3 sill, almandine–pyrope, eclogitic paragenesis										
012	39.45	0.66	21.78	0.04	17.14	0.32	9.83	9.49	0.09	98.80
Candado Julio sill, almandine–pyrope, eclogitic paragenesis										
006a	39.89	0.57	22.13	0.09	16.19	0.19	13.89	5.56	0.16	98.67
Bicicleta sill, almandine–pyrope, eclogitic paragenesis										
004	39.97	0.55	21.48	0.01	18.48	0.31	10.96	7.01	0.20	98.97
Quebrada Grande placer, almandine–pyrope, eclogitic paragenesis										
V-6	40.91	0.56	22.21	0.08	15.66	0.33	14.16	5.39	0.23	99.53
V-7	40.92	0.54	22.32	0.14	15.87	0.20	13.29	6.14	0.20	99.62
V-9	40.57	0.60	22.04	0.07	17.49	0.34	10.09	8.38	0.24	99.82
V-12	41.23	0.77	21.42	0.29	15.16	0.35	16.18	4.56	0.04	100.00
V-14	40.27	0.50	21.75	0.04	18.20	0.24	10.52	8.08	0.23	99.83
V-16	40.49	0.55	21.96	0.05	17.42	0.35	10.31	8.50	0.19	99.82
V-18(1)	40.05	0.57	22.09	0.04	17.04	0.36	8.92	10.62	0.26	99.95
V-18(2)	40.53	0.64	21.85	0.14	16.07	0.50	10.60	9.13	0.18	99.64
V-19	39.85	0.65	21.97	0.11	16.87	0.34	10.53	9.39	0.24	99.95
V-24	40.24	0.70	21.78	0.07	16.98	0.45	8.34	11.06	0.31	99.93
V-25	39.49	0.65	21.72	0	17.37	0.35	7.03	12.85	0.12	99.58
V-26(1)	39.99	0.68	21.91	0	16.89	0.49	10.20	9.57	0.18	99.91
V-26(2)	39.98	0.68	21.79	0	17.07	0.52	10.08	9.56	0.24	99.92
V-27	39.39	0.75	21.97	0.04	17.24	0.78	8.32	11.17	0.28	99.94
V-30	41.19	0.45	22.40	0.09	15.57	0.28	13.91	5.39	0.19	99.47
V-32	41.02	0.53	22.28	0	15.79	0.24	13.86	5.40	0.18	99.30
Quebrada Grande placer, pyrope, peridotitic paragenesis										
V-1*	40.83	0.16	12.60	13.75	6.16	0.28	20.01	5.63	0	99.42
V-2*	41.60	0	17.09	9.88	6.45	0.49	23.21	0.88	0	99.60
V-36(1)	41.36	0.04	18.11	6.90	6.42	0.29	20.34	5.62	0	99.08
V-36(2)	41.74	0.01	18.13	6.88	6.68	0.36	20.31	5.71	0	99.82
La Centella placer, almandine–pyrope, eclogitic paragenesis										
1448*	39.81	0.62	22.04	0.02	16.41	0.15	10.24	9.60	0	98.89
1504*	40.34	0.59	21.83	0.04	17.39	0.26	12.25	6.78	0.05	99.53
1810	40.05	0.56	21.41	0.02	18.40	0.26	12.04	6.57	0	99.31
1877*	39.95	0.57	22.15	0.02	17.27	0.29	10.01	9.07	0.23	99.56
1991*	40.16	0.50	22.18	0	15.00	0.22	9.18	12.40	0.28	99.92
2138	39.15	0.62	21.87	0.06	15.66	0.30	8.38	12.48	0.35	98.87
2212	39.79	0.42	21.58	0	18.81	0.46	9.95	8.14	0.16	99.31
2214*	40.29	0.61	21.82	0.14	17.77	0.40	12.17	6.66	0.12	99.98
2220	40.88	0.59	22.36	0.12	15.06	0.26	11.25	8.66	0.26	99.44

* Garnet analyzed for trace elements with LAM–ICP–MS. Compositions are expressed in wt.% oxides.

Omphacitic clinopyroxene is relatively common as an inclusion in diamond at Guaniamo. In some cases, composite pyroxene and garnet inclusions are observed. In total, 34 clinopyroxene inclusions were analyzed (12 grains extracted from diamond from sills, 12 from diamond from the Quebrada Grande placer, and 10 from diamond from the La Centella placer). Results are presented in Table 10. Figure 9 shows the Mg–Ca–Fe proportions of the pyroxene; these all fall within a restricted field, except for one outlier (#012a), with a higher Fe content (13% FeO).

Na contents vary from 3.63 to 7.46 wt.% Na_2O, which corresponds to 25 to 51 mol.% jadeite component. Al contents vary from 7.21 to 13.53 wt.% Al_2O_3, and are positively correlated with Na. The pyroxene inclusions have high concentrations of K (0.2–1.4 wt.% K_2O), which generally are negatively correlated with Na contents (Fig. 12). For the most part, the Na and K contents of clinopyroxene included in Venezuelan diamond are intermediate between those of inclusions in diamond from Argyle and Arkhangelsk, and the K-poor clinopyroxene inclusions in diamond from other pipes in the world (Fig. 12).

The trace-element patterns of the clinopyroxene inclusions (Fig. 10C) are characterized by mild enrichment in the *LREE*, and depletion in the *HREE*, compared to the included garnet. Their Sr contents (300–500 ppm) are somewhat higher than in most examples of clinopyroxene from both diamondiferous and barren eclogite xenoliths, but lower than most of the values reported for clinopyroxene from Argyle (Griffin *et al*. 1988, Fig. 13). However, most of the analyzed clinopyroxene inclusions at Guaniamo have unusually high Zr contents (>50 ppm).

Diamond crystals that contain orange garnet and omphacite inclusions also commonly enclose inclusions of a colorless mineral, which, in diamond characterized by the E-type paragenesis, is probably *coesite*.

Compositional data for *rutile* inclusions in diamond from one sill and from the Guaniamo placer are presented in Table 11. These rutile inclusions have similar compositions, which are typical of E-type inclusions of rutile in diamond.

Ilmenite inclusions were found in four diamond crystals (Table 11). Ilmenite in diamond from other areas worldwide is commonly very rich in both Mg and Cr. In contrast, the ilmenite inclusions from the Guaniamo area have low Mg contents, from 0.30 to 0.44 wt.% MgO. Inclusions of Mg-poor ilmenite have been found previously in only two other of diamond crystals, both from Brazil (Meyer & Svisero 1975). The ilmenite studied here also has high Mn contents (0.91–1.04 wt.% MnO). Recently, similar inclusions of manganoan ilmenite have been found associated with ferroan

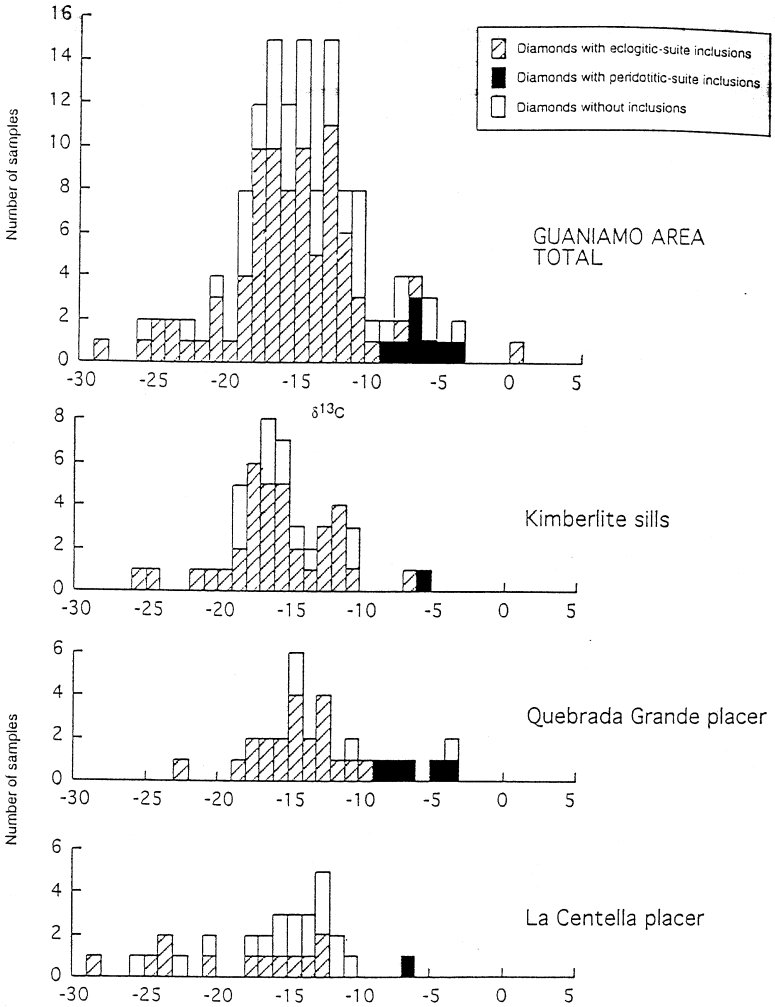

FIG. 8. Distribution of $\delta^{13}C$ values in diamond from the Guaniamo area. The majority of diamond crystals are isotopically light, with $\delta^{13}C < 10‰$. In addition to diamond from Quebrada Grande and La Centella placers, diamond samples from other localities are included in the total histogram.

periclase in diamond from the Juina area, Brazil, and interpreted as a member of the superdeep assemblage (see below) (Kaminsky *et al.* 2001). The low-Mg, high-Mn ilmenite in diamond at Guaniamo also may belong to the superdeep association.

Sulfides were also found included in diamond from the Guaniamo suite. The low Ni contents (0.29–1.46%; Table 12) suggests that they form part of the eclogitic paragenesis (Bulanova *et al.* 1996).

Six crystals or fragments of diamond have coexisting garnet and clinopyroxene inclusions. Equilibrium temperatures and pressures for these mineral pairs were calculated using the Ellis & Green (1979) geothermometer, and a version of this thermometer modified for Na in garnet and the Ca-Tschermak substitution in clinopyroxene (Simakov 1996, and unpubl. data). The latter approach also allows a pressure estimate. For most samples, the T estimates agree within the probable errors of each method (±50°C). Where P estimates could be obtained by the Simakov method, these lie in the deeper part of the lithospheric mantle.

The Ellis and Green temperatures of these crystals of diamond (calculated at 55 kbar) range from 1025 to 1450°C (Table 13). The mean value, ignoring the highest and lowest values, is 1182°C. This is approximately 75°C lower than the mean temperature of 13

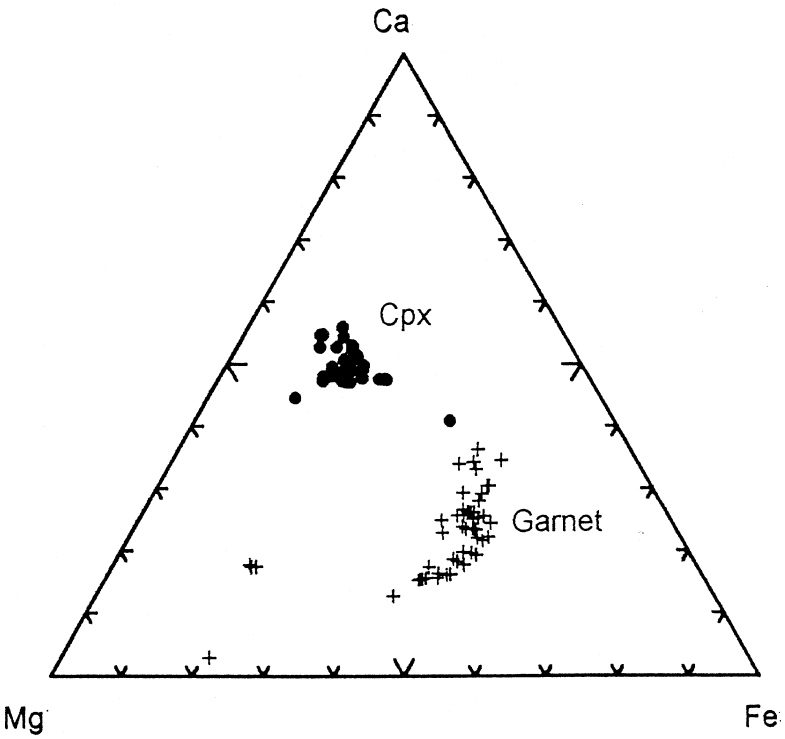

FIG. 9. Composition of garnet and clinopyroxene included in diamond at Guaniamo, in terms of Mg–Ca–Fe (at.%).

clinopyroxene–garnet pairs from Argyle, calculated in the same way (Griffin *et al*. 1989). Whereas we were unable to determine the trace-element patterns of the coexisting phases because of grain-size constraints, the overall pattern of relative abundances of elements in the garnet and clinopyroxene can give an indication of relative temperature. Griffin *et al*. (1989) showed that the value of $D_{Zr}^{cpx/grt}$ decreases with increasing T, whereas $D_{Ga}^{cpx/grt}$ increases. The clinopyroxene inclusions of the Guaniamo suite have generally higher Zr than those of the Argyle suite, whereas the garnet inclusions have lower Zr contents than the corresponding garnet at Argyle. In contrast, the Ga contents of the clinopyroxene at Guaniamo and Argyle are similar, whereas the garnet at Guaniamo has significantly lower mean Ga contents than the Argyle garnet (15 ppm *versus* 25 ppm). These data are consistent with a lower mean temperature of formation of the eclogitic diamond at Guaniamo, compared to that in the Argyle suite.

The peridotitic paragenesis

Inclusions of the *peridotitic paragenesis* include chromian pyrope, chromian spinel, and olivine.

Chromian pyrope. Although subcalcic garnet of the harzburgite–dunite suite is prevalent among chromian pyrope inclusions in diamond worldwide, it is rare in diamond from sills and placers of the Guaniamo district (Fig. 14). Four crystals of chromian pyrope have been found in three crystals of diamond from the Guaniamo placers (Table 8). All of these pyrope inclusions are enriched in the knorringite component (6.9 to 13.8 wt.% Cr_2O_3), with low iron contents (13.5–15.0 wt.% FeO). Two of them fall within the lherzolite field, and two within the harzburgite field (Fig. 14). Nixon *et al*. (1995) have described other inclusions of subcalcic pyrope typical of a lherzolitic association in diamond at Guaniamo.

The trace-element patterns of two of the garnet inclusions are shown in Figure 10B. They show sinuous *REE* patterns, with a depletion (relative to Sc) in the *HREE* and an enrichment in the middle rare-earth elements, giving a peak near Nd. This pattern, defined by high Sc/Y and Nd/Y, is characteristic of chromian pyrope in diamond worldwide and is interpreted to reflect metasomatism associated with diamond formation (Shimizu & Richardson 1987, Griffin *et al*., unpubl. data). The nickel-based temperatures (Ryan & Griffin

TABLE 9. TRACE-ELEMENT CONCENTRATIONS IN MINERALS INCLUDED IN DIAMOND AT GUANIAMO

Mineral	Garnet Eclogite paragenesis								Pyrope		Omphacitic Clinopyroxene						
Sample	014	1448	1504	1877	1877-bis	1991	2214	V-1	V-2	PHN 5921*	012	012a	018	019	063a	063b	1815
Sc ppm	50	53	55	56	60	41	62	211	219	106	15	<12.26	<14.16	21	22	25	18
Ti	3270	4505	7704	3480	3525	4140	3402	992	62	800	1422	960	3198	3081	1416	2789	1614
V	166	235	339	195	200	190	190	474	287	270	371	215	196	190	394	225	532
Co	31	24	67	49	47	33	66	45	46	39	30	18	15	11	23	16	14
Ni	<14.57	12	19	<29.39	33	20	43	118	121	84	86	68	63	31	40	138	16
Ga	16	53	19	13	15	14	14	7	3	na	22	14	13	13	21	25	35
Sr	26.5	12.4	8.5	6.8	6.4	9.1	5.6	22.7	10.7	0.5	310.2	556.8	285.8	303.5	461.9	452.4	375.9
Y	43.1	45.8	36.3	40.1	54.6	48.4	45.2	4.6	4.2	2.5	3.3	3.9	<1.55	1.4	3.0	9.6	2.8
Zr	18.8	35.5	66.1	12.6	17.1	40.9	49.9	17.2	4.6	11.0	23.6	19.0	75.5	55.6	75.9	95.8	23.9
Nb	<1.13	1.10	<1.21	<2.41	3.65	<1.62	1.06	0.57	0.70	0.16	<0.74	<1.46	<2.40	<1.99	1.70	<2.47	1.44
La	<0.64	0.58	<0.74	1.49	<0.69	<0.98	1.14	2.29	1.15	0.04	4.96	3.55	5.07	<1.29	1.16	5.36	4.90
Ce	<0.59	4.18	1.94	1.91	2.14	<0.73	7.47	5.28	4.80	0.22	5.28	11.40	13.43	6.30	6.21	33.22	3.68
Pr	<0.49	1.40	<0.73	3.23	0.49	<0.54	1.09	1.03	0.83	0.09	0.72	2.70	2.24	<0.74	1.49	3.00	3.18
Nd	<3.32	5.41	7.10	7.50	<2.56	<4.05	4.48	7.85	2.78	0.68	5.17	11.64	<5.26	<4.70	7.99	19.68	5.24
Sm	3.04	3.89	6.27	<3.26	3.57	4.57	2.02	2.43	1.09	0.43	<1.77	<3.88	<3.52	<3.76	1.89	<3.18	1.88
Eu	2.52	1.98	<1.18	<2.32	<0.83	1.61	0.97	0.32	<0.40	0.15	<0.56	<1.45	<1.83	<1.59	0.61	2.07	<0.76
Gd	6.25	5.25	4.25	3.48	5.28	6.84	4.28	0.95	0.76	0.45	<1.59	<3.89	<4.16	<3.02	1.66	<3.57	<1.42
Dy	6.29	6.38	5.62	9.91	9.41	10.39	6.26	0.82	<1.23	0.53	<2.31	<4.55	6.20	<4.45	3.13	<5.39	<1.84
Ho	2.03	1.66	1.02	1.19	1.82	1.69	1.71	0.17	<0.22	0.95	<0.41	<0.78	<1.16	<0.71	<0.20	<0.88	<0.30
Er	6.57	5.81	5.26	3.33	6.10	7.11	4.74	<0.49	1.00	0.28	<1.20	<2.62	<2.47	<2.37	<0.50	<3.08	<0.93
Yb	4.27	4.91	4.80	6.77	9.30	3.94	5.99	0.55	1.94	0.40	<0.93	<2.09	<2.56	<2.11	<0.37	<2.86	<0.84
Lu	<0.50	0.94	0.72	<1.29	1.45	<0.82	0.76	0.18	0.27	0.09	<0.31	<0.71	<0.85	<0.59	<0.15	<0.86	<0.49
Hf	<1.92	1.15	3.85	<3.10	<1.43	<1.69	1.61	0.80	<0.56	0.32	<1.13	<3.41	3.61	<3.29	4.24	<2.45	<1.25

* Locality unknown.

1996) of these two garnet inclusions are similar (1380 and 1395°C), and that of sample PHN5921 is lower (1225°C). All the temperatures are within the range estimated independently for the eclogitic parageneses discussed earlier.

Olivine. Five inclusions of olivine were analyzed, two of which are from a single crystal of diamond from one of the sills; the other three grains were extracted from two crystals of diamond from the Quebrada Grande placer. All the olivine inclusions have similar forsterite contents (93–94.5%) and contain insignificant amounts of Cr (0.04–0.08 wt.% Cr_2O_3) and Ca (0.01 wt.% CaO); Ni contents are in the normal range for mantle olivine (0.33–0.39 wt. % NiO). Olivine inclusions in diamond from the Guaniamo area are thus similar in major-element composition to olivine inclusions in diamond from other regions worldwide. One crystal of olivine (#040–1) was analyzed for trace elements, yielding values for V (27 ppm), Cr (890 ppm), Mn (812 ppm) and Co (143 ppm), within the range of other estimates of the composition of mantle olivine.

Chromian spinel (*chromite*) was found in three crystals of diamond from the Quebrada Grande placer and in one from the La Centella placer. Compositions are presented in Table 11. These inclusions of chromian spinel have Cr and Al contents ranging from 63.6 to 66 wt.% Cr_2O_3 and 6.76 to 7.25 wt.% Al_2O_3, respectively, which is typical for chromian spinel inclusions in diamond from the majority of diamond deposits worldwide. Most chromian spinel from alluvium in the Guaniamo area and from sills have Cr contents that are similar to those of chromian spinel inclusions in diamond, except for their commonly lower Mg and higher Fe contents (Table 11).

The superdeep paragenesis

The superdeep paragenesis may be represented by one inclusion of ferroan periclase found in a diamond crystal from the Quebrada Grande placer deposit (#V–40). Ferroan periclase and perovskite-structured $CaSiO_3$ and $MgSiO_3$ represent the high-pressure mineral assemblage expected in mantle peridotite at depths greater

TABLE 10. COMPOSITION OF CLINOPYROXENE INCLUDED IN DIAMOND AT GUANIAMO

Sample	SiO_2	TiO_2	Al_2O_3	Cr_2O_3	FeO	MnO	MgO	CaO	Na_2O	K_2O	Total
Los Indios sill											
001 wt.%	56.05	0.65	13.41	0.10	3.28	0.08	8.24	10.31	7.46	0.36	99.94
Area 024/1 sill											
018*	53.75	0.63	9.66	0	4.15	0.03	9.42	17.19	3.63	0.96	99.42
019*	54.49	0.56	9.50	0.03	4.42	0.04	9.59	16.71	3.75	0.88	99.97
037c	54.82	0.66	12.89	0	4.02	0.10	7.55	13.04	6.23	0.67	99.98
060	55.48	0.56	11.92	0	3.68	0.06	8.53	13.63	5.42	0.68	99.96
063a*	55.99	0.30	10.16	0.04	5.11	0.06	8.92	13.62	5.05	0.66	99.91
063b*	56.34	0.53	7.21	0.09	3.75	0.06	13.00	13.40	5.04	0.23	99.65
064a	56.55	0.27	11.32	0.02	4.41	0	8.66	12.57	5.45	0.72	99.97
Area 024/3 sill											
010a	55.13	0.54	8.41	0.04	5.39	0.07	10.71	14.39	4.57	0.71	99.96
012*	55.69	0.23	9.91	0.01	5.47	0.12	8.83	13.62	5.26	0.65	99.79
012a*	53.56	0.17	5.01	0.03	13.10	0.07	8.35	14.84	3.34	1.38	99.85
013	55.62	0.73	12.63	0.02	4.43	0.04	7.61	11.66	6.14	0.69	99.57
Quebrada Grande placer											
V-8	54.57	0.16	8.63	0.03	5.34	0.11	9.74	16.31	3.88	0.84	99.61
V-11	55.11	0.71	9.91	0.05	4.69	0.05	8.76	14.51	5.01	1.14	99.94
V-17(1)	54.95	0.27	8.22	0.04	5.43	0.02	10.61	15.10	4.43	0.71	99.78
V-17(2)	55.01	0.27	8.25	0.06	5.32	0.11	10.74	14.91	4.21	0.75	99.63
V-19	55.50	0.26	7.82	0.08	5.35	0.06	10.17	15.21	4.09	0.80	99.34
V-20	56.27	0.39	9.35	0.08	4.12	0.08	10.48	13.49	4.95	0.78	99.99
V-21(1)	54.48	0.58	8.71	0.08	5.16	0.10	9.64	16.50	3.84	0.81	99.90
V-21(2)	55.02	0.56	8.26	0.07	5.59	0.04	9.62	15.96	3.94	0.75	99.81
V-22	56.20	0.68	13.34	0.09	3.62	0.15	7.94	10.74	6.55	0.40	99.71
V-23	55.59	0.27	11.26	0.05	5.12	0.01	8.06	13.08	5.79	0.77	100.00
V-25	56.50	0.23	13.53	0.11	3.42	0	7.88	10.43	7.02	0.45	99.57
V-29	56.54	0.22	13.49	0.10	3.36	0.15	7.87	11.08	6.70	0.35	99.86
La Centella placer											
1448	55.48	0.74	13.10	0.09	4.02	0.01	7.44	10.84	7.41	0.69	99.82
1451	55.32	0.77	9.65	0.09	5.67	0.10	8.90	13.29	5.27	0.69	99.75
1504	55.05	0.54	7.63	0.04	5.89	0.09	10.57	14.65	4.61	0.75	99.82
1518	55.21	0.23	8.02	0.03	5.59	0.13	10.69	14.91	4.33	0.67	99.81
1815*	55.22	0.25	10.08	0.03	4.67	0.04	9.19	14.32	5.17	0.79	99.76
1877	55.63	0.22	10.38	0.03	4.54	0	9.18	14.15	5.16	0.75	100.04
2089	55.20	0.78	10.77	0.09	4.78	0.06	8.62	13.09	5.91	0.66	99.96
2127	55.24	0.36	9.24	0.07	5.26	0.12	9.32	14.31	5.08	0.91	99.91
2208	55.15	0.63	9.76	0.07	4.94	0.01	8.71	14.36	5.18	1.04	99.85
2217	55.43	0.24	13.31	0.05	4.18	0.15	7.24	12.09	6.83	0.57	100.09

* Clinopyroxene analyzed for trace elements with LAM–ICP–MS. Compositions are expressed in wt.% oxides.

TABLE 11. COMPOSITION OF OPAQUE MINERALS INCLUDED IN DIAMOND AT GUANIAMO

Location	Sample	TiO_2	Al_2O_3	Cr_2O_3	FeO	MnO	MgO	Total
Rutile								
Area 024/1 sill	055	98.87	0.59	n.d.	0.31	0	0.07	99.84
Quebrada Grande placer	V-37	98.49	0.69	0.05	0.68	0.05	0	99.96
Ilmenite								
Area 024/1 sill	039	51.35	0.07	0.05	46.46	0.91	0.34	99.18
Quebrada Grande placer	V-15(1)	50.63	0.12	0.02	47.53	1.04	0.33	99.67
Quebrada Grande placer	V-15(2)	49.99	0.08	0.05	47.37	1.01	0.44	98.94
Quebrada Grande placer	V-33(1)	50.82	0.12	0.04	46.16	0.99	0.30	98.43
Chromian spinel								
Quebrada Grande placer	V-4	0.09	6.76	66.15	11.43	0.36	14.68	99.47
Quebrada Grande placer	V-13	0.16	6.87	65.74	11.69	0.29	14.88	99.63
Quebrada Grande placer	V-38	0.34	7.12	63.84	11.83	0.26	15.81	99.20
La Centella placer	1812	0.36	7.25	63.61	12.11	0.26	16.03	99.62
Ferroan periclase								
Quebrada Grande placer	V-40	n.d.	n.d.	0.15	19.42	n.d.	80.12	99.69

Compositions are expressed in wt.%; n.d.: not detected.

than the transition zone (= 660 km). This assemblage has been described in diamond from several localities worldwide, and is accepted as indicating the derivation of such diamond from lower-mantle depths. The occurrence of ferroan periclase alone does not require unusually high pressure, and does not prove derivation from such depths. However, the composition of the ferroan periclase [Mg/(Mg + Fe) = 0.88; Table 12] at Guaniamo is similar to that of ferroan periclase inclusions in diamond from most other localities worldwide (Harte *et al*. 1999, Davies *et al*. 1999). The ratio is higher than that of most examples of ferroan periclase reported from Brazil (Harte *et al*. 1999, Kaminsky *et al*. 2001). We tentatively hypothesize, therefore, that the ferroan periclase inclusion represents the superdeep paragenesis.

Discussion

The mineral inclusions in diamond at Guaniamo are predominantly (approximately 85%) of the eclogitic paragenesis, and there is a good correlation between paragenesis, as defined by mineral inclusions, and carbon-isotope composition. If this correlation is extended to the diamond crystals for which only carbon-isotope data are available, including those reported by Galimov *et al.* (1999), it implies that 90–95% of the diamond in the Guaniamo suite was derived from eclogitic host-rocks. This estimate places the Guaniamo deposits among a small group of diamond deposits worldwide that are strongly dominated by eclogite-derived diamond. These include the Argyle lamproite (Jaques *et al.* 1989), the Orapa pipe (Gurney *et al*. 1984, Deines *et al.* 1993), the Premier mine (Gurney *et al*. 1985) and some pipes of the Arkhangelsk region (Zakharchenko *et al*. 1991) and the Slave Craton (Davies *et al*. 1999).

P–T calculations, based on coexisting clinopyroxene + garnet pairs in the diamond yield mean temperatures of about 1180°C according to the Ellis and Green method, or about 1145°C by the Simakov method (ignoring one extremely low value). High temperatures (1250–1400°C) are also implied by the high Ni contents of the three chromian pyrope inclusions for which data

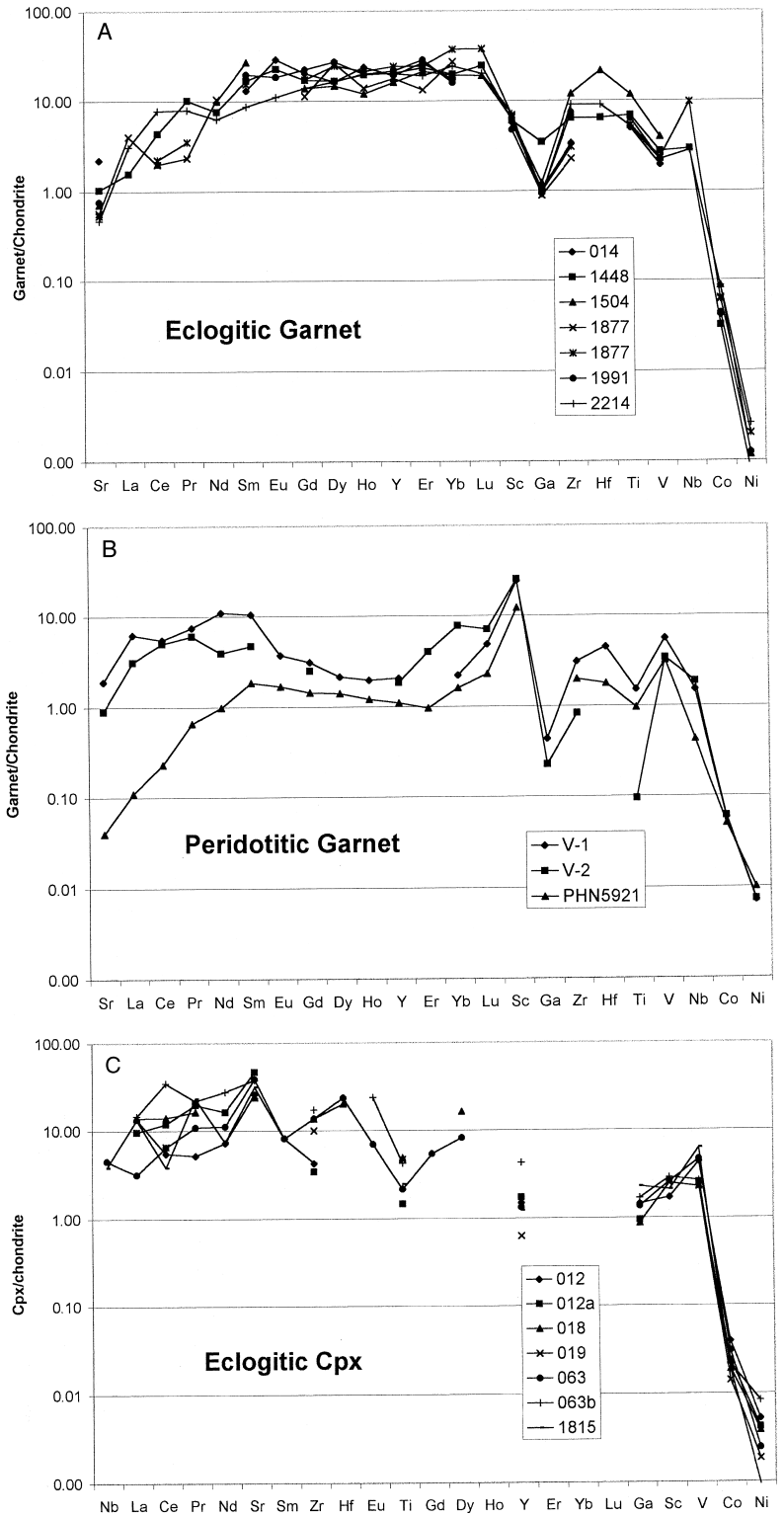

FIG. 10. Trace-element distribution in (A) garnet from an eclogite paragenesis, (B) garnet from a peridotitic paragenesis, and (C) omphacite clinopyroxene, included in diamond in the Guaniamo suite.

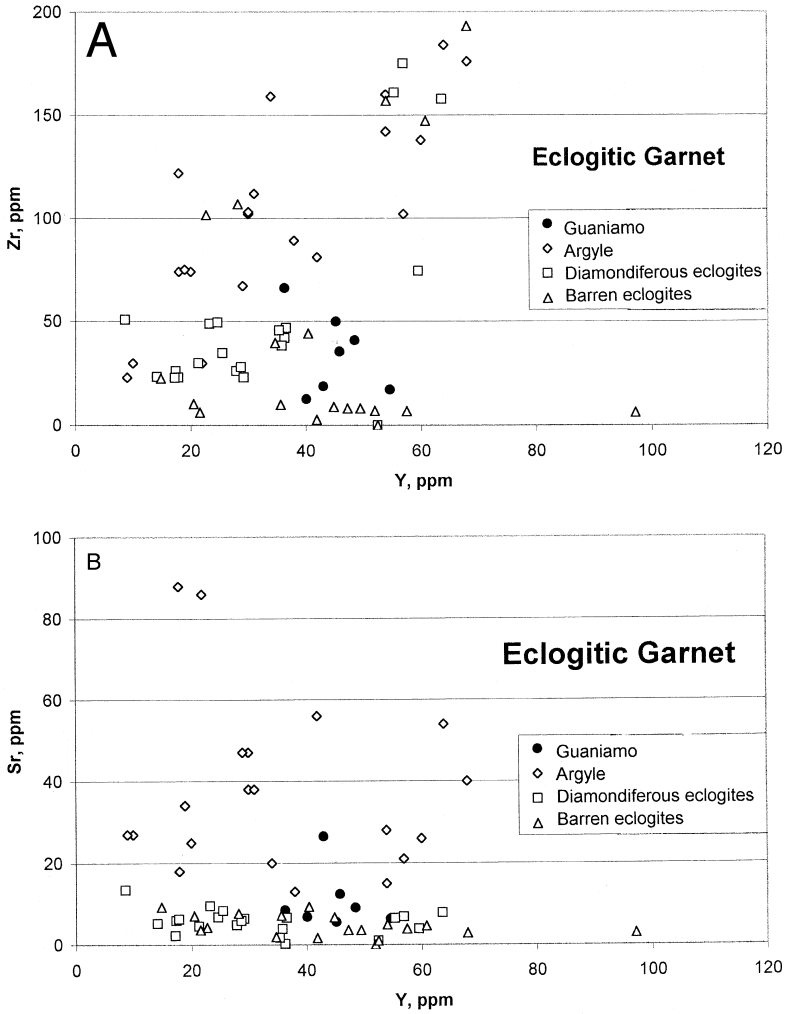

FIG. 11. Characteristics of trace elements in garnet from an eclogitic paragenesis included in diamond at Guaniamo: (A) Zr *versus* Y, and (B) Sr *versus* Y.

are available. These high temperatures are consistent with the data on the state of aggregation of nitrogen impurities in the diamond. The degree of aggregation from A to B centers is a function of temperature, time, and nitrogen content (Mendelssohn & Milledge 1995, Taylor *et al.* 1996). The relatively high degree of aggregation observed in these crystals of relatively low-N diamond therefore suggests that they have been stored at high temperatures in the mantle prior to eruption. However, the aggregation process is also enhanced by strain on the diamond, evidence for which is exhibited as plastic deformation lamellae. Their presence makes it difficult to make quantitative estimates of temperature–time relationships.

TABLE 12. COMPOSITION OF SULFIDES INCLUDED IN DIAMOND AT GUANIAMO

Sample	Fe	Ni	Cu	As	Se	S	Total
			Area 024/1 sill				
056	58.18	1.46	0.87	0	0.13	39.30	99.94
			Quebrada Grande placer				
V-12(1)	59.13	0.29	0.45	0.06	0.08	39.81	99.82
V-12(2)	59.83	0.30	0.23	0	0.09	39.55	100.00

Compositions are quoted in wt.%.

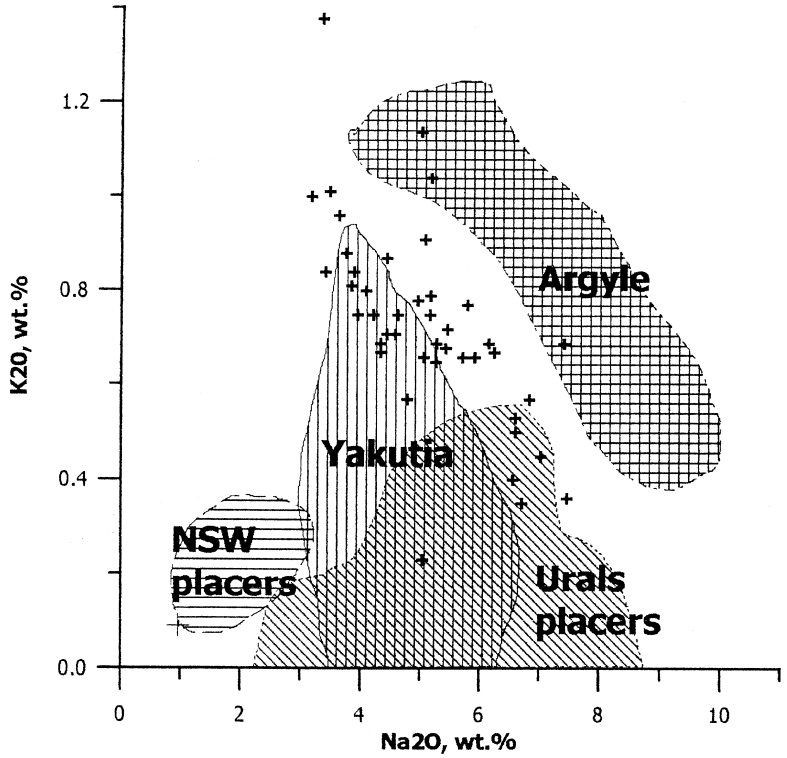

FIG. 12. Plot for Na_2O *versus* K_2O for pyroxene inclusions in diamond at Guaniamo (crosses), Argyle pipe, New South Wales placers, Yakutian pipes and the Urals placers.

TABLE 13. TEMPERATURE ESTIMATES FOR GARNET–CLINOPYROXENE PAIRS INCLUDED IN DIAMOND AT GUANIAMO (ECLOGITIC PARAGENESIS)

Sample	Location	P, kbar	T, °C	T, °C at 55 kbar
012	Area 024/3 sill	60.4	1065	1450
V-19	Quebrada Grande placer	61.5	1212	1189
V-25	Quebrada Grande placer	52.4	1021	1025
1448	La Centella placer	56.8	1218	1212
1504	La Centella placer	55.4	1205	1203
1877	La Centella placer	56.9	974	1122

Pressure and temperature estimates made using the approach of Simakov (1996). The estimate of temperature of equilibration for a pressure of 50 kilobars is based on the data of Ellis & Green (1979).

TABLE 14. COMPOSITION OF OLIVINE INCLUDED IN DIAMOND AT GUANIAMO

Sample	SiO_2	Cr_2O_3	FeO	NiO	MgO	CaO	Total
			Area 024/1 sill				
040(1)	41.61	0.05	5.85	0.33	51.59	0.01	99.44
040(2)	41.44	0.08	6.38	0.37	51.59	0.01	99.87
			Quebrada Grande placer				
V-5(1)	41.80	0.06	5.79	0.39	51.70	0.01	99.75
V-5(2)	41.73	0.04	5.47	0.36	52.16	0.01	99.77
V-28	41.21	0	6.35	0.37	51.63	0	99.56

Compositions are reported in wt.% oxides.

Whereas no data are available on the paleogeotherm beneath the Guaniamo area, Griffin & Ryan (1995) have shown that the base of the depleted lithosphere beneath cratonic areas typically lies at temperatures of 1250–1350°C. The high temperatures of the diamond inclusions suggest that all of the diamond crystals were derived from near the base of the lithosphere beneath the Western Guyana Shield. At these depths, eclogites may be an important rock-type, mixed into a peridotitic mantle consisting of both harzburgite and lherzolite.

The data presented here show remarkable similarities between the Guaniamo suite and diamond recovered from the Argyle lamproite. These include: (1) very high proportions of eclogite-paragenesis diamond,

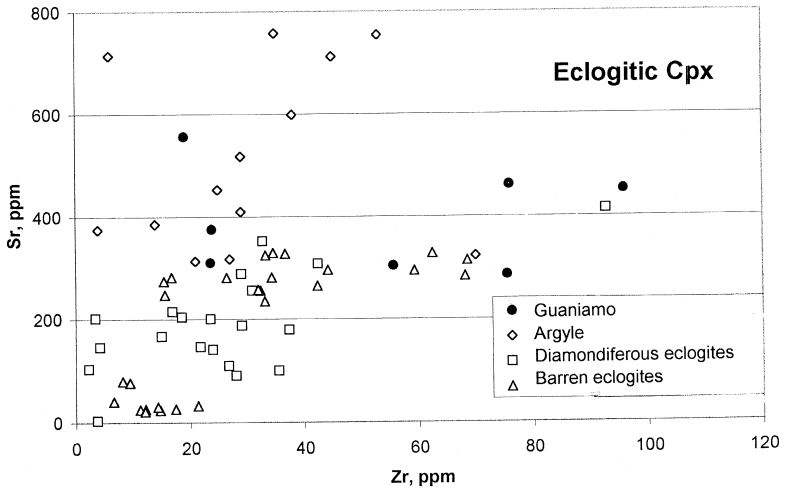

FIG. 13. Characteristics of trace elements in omphacitic clinopyroxene included in diamond at Guaniamo: Sr *versus* Zr.

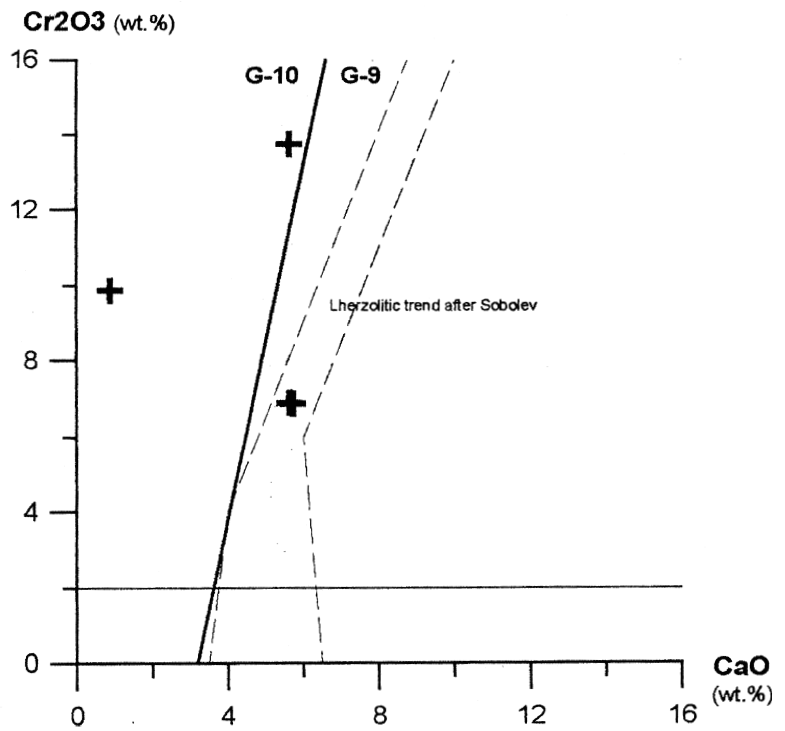

FIG. 14. Plot of CaO *versus* Cr_2O_3 for pyrope included in diamond at Guaniamo.

(2) very high mean temperatures of diamond formation, (3) high levels of Ti and Na in garnet, and Ti and K in clinopyroxene included in diamond (Jaques *et al*. 1989, Griffin *et al*. 1989). The association of both deposits with magmas that intruded Proterozoic cratons, rather than typically Archean cratons, within a relatively short time (<1 Ga) after the last major tectonothermal event, may be significant. The prevalence in both localities of eclogitic diamond with isotopically light carbon, and mineral inclusions suggesting a peraluminous host-rock, may indicate that the addition of crustal rocks to the base of the lithosphere was an important feature of Proterozoic tectonics.

The abundance of green, rather than brown, radiation spots, and the low level of abrasion on most crystals of diamond, suggest that most of the diamond crystals in the placers have had a short crustal history, and probably have been transported over distances no greater than 10–20 km. The morphology and other features of the diamond from the Quebrada Grande placer are consistent with their derivation almost entirely from the known sills of kimberlite.

The Ringi–Ringi and Chihuahua alluvial deposits differ from the Quebrada Grande deposit and the known sills in that they have higher proportions of green and yellow diamonds, transparent and unjointed diamonds, and diamond with blue luminescence. Their curves of nitrogen-impurity distribution (Fig. 7) are similar to those for diamond of the Quebrada Grande deposit and the kimberlite sills. It seems likely that the diamond in the Ringi–Ringi and Chihuahua deposits has been derived in part from kimberlite sills that remain to be discovered. However, it seems most probable that the diamond of all these placers has been derived from local kimberlites, and not from the ancient Roraima sediments as earlier supposed.

The La Centella placer is geomorphologically isolated from the known kimberlite sills, but its diamond population also bears little evidence of long transport. This finding suggests that they have been supplied from a different, as yet undiscovered body of kimberlite. This supposition is supported by their nitrogen-impurity distribution curve, which is significantly different from those for the other deposits.

Conclusions

1. Essentially all of the diamond in the Guaniamo placer deposits is of local origin, and has been derived from kimberlite sills, rather than having been recycled from ancient sediments. Variations in characteristics of the diamond crystals from various deposits suggest that some have been derived from kimberlites that remain to be discovered.

2. Most mineral inclusions in the diamond at Guaniamo are of the eclogitic paragenesis, and were likely derived from peraluminous mafic rocks. Significant numbers of inclusions of a peridotitic (lherzolitic and harzburgitic) association *e.g.,* chromian pyrope, chromian spinel, olivine, also have been found. One inclusion of ferroan periclase may represent the superdeep paragenesis, derived from the lower mantle.

3. Most of the diamond from an eclogitic association has isotopically light carbon ($\delta^{13}C$ from –10 to –25‰), whereas the diamond from a peridotitic association is isotopically heavier ($\delta^{13}C$ from –3 to –9‰). On this basis, we estimate that 93 ± 2% of the diamond at Guaniamo belongs to the eclogitic paragenesis.

4. P–T estimates on mineral inclusions suggest that most are derived from near the base of the lithosphere (T 1200–1300°C). This zone may contain a substantial proportion of eclogite formed by subduction of crustal material.

5. The very high proportion of diamond from an eclogitic association in the Guaniamo deposits, and several features of the mineral inclusions in the diamond, show striking parallels to the Argyle deposit of Australia; both deposits occur within cratons that have experienced extensive Proterozoic tectonothermal activity.

Acknowledgements

We thank the Guaniamo Mining Company, and in particular Mr. Robert Cooper, for supporting this research and allowing the publication of this work. We thank Peter Nixon for providing garnet PHN5190, Esme van Achterbergh for carrying out most of the trace-element analyses, and Prof. S. O'Reilly for extremely valuable support in organizing the research. We thank Robert F. Martin, Tom McCandless and an anonymous reviewer for thoughtful and constructive reviews, which improved the manuscript. Parts of this work were supported by ARC grants to WLG.

References

Baptista, G.J. & Svisero, D.P. (1978): Geologia de los depositos diamantiferos de la parte norooccidental de la Guayana Venezolana. *Republica de Venezuela, Ministerio de Energia y Minas, Boletin de Geologia* **13**(24), 3-46.

Boyd, S.R., Kiflawi, I. & Woods, G.S. (1994): The relationship between infrared absorption and the A defect concentration in diamond. *Phil. Mag.* **B69**, 1149-1153.

_____, _____ & _____ (1995): Infrared absorption by the B nitrogen aggregate in diamond. *Phil. Mag.* **B72**, 351-361.

Bulanova, G.P., Griffin, W.L., Ryan, C.G., Shestakova, O.Y. & Barnes, S.-J. (1996): Trace elements in sulfide inclusions from Yakutian diamonds. *Contrib. Mineral. Petrol.* **124**, 111-125.

Channer, D.M.DeR., Cooper, R. & Kaminsky, F. (1998): The Guaniamo diamond region, Bolivar state, Venezuela: a new kimberlite province. *In* Seventh International Kimberlite Conference (Cape Town), Extended Abstr. (144-146).

CURTIS, G.E. (1975): Venezuela's Valley of Diamonds: El Guaniamo Diamond Shout. *Lapidary J.*, February 1975, 1708-1718.

DAVIES, R., GRIFFIN, W.L., PEARSON, N.J., ANDREW, A.S., DOYLE, B.J. & O'REILLY, S.Y. (1999): Diamonds from the deep: Pipe DO–27, Slave Craton, Canada. *In* Proc. VIIth Int. Kimberlite Conf. **1** (J.J. Gurney, J.L. Gurney, M.D. Pascoe & S.H. Richardson, eds.). Red Roof Design, Cape Town, South Africa (148-155).

DEINES, P. (1992): Mantle carbon: concentration, mode of occurrence, and isotopic composition. *In* Early Organic Evolution: Implications for Mineral and Energy Resources (M. Schidlowski et al. eds.). Springer-Verlag, Berlin, Germany (133-146).

_____, HARRIS, J.W. & GURNEY, J.J. (1993): Depth-related carbon isotope and nitrogen concentration variability in the mantle below the Orapa kimberlite, Botswana, Africa. *Geochim. Cosmochim. Acta* **53**, 2781-2796.

ELLIS, D.J. & GREEN, D.H. (1979): An experimental study of the effect of Ca upon garnet–clinopyroxene Fe–Mg exchange equilibria. *Contrib. Mineral. Petrol*. **71**, 13-22.

GALIMOV, E.M. (1968): *Geochemistry of Stable Carbon Isotopes*. Izd. Nedra, Moscow, Russia (in Russ.).

_____, KAMINSKY, F.V., GRICICK, V.V. & IVANOVSKAYA, I.N. (1978): Carbon isotope composition of diamonds from placers. *In* Short papers of the Fourth International Conference on Geochronology, Cosmochronology, Isotope Geology. *U.S. Geol. Surv., Open-File Rep.* **78-701**.

_____, SOBOLEV, N.V., YEFIMOVA, E.S. & SHIRYAEV, A.A. (1999): Carbon isotopic composition of Venezuelan diamonds. *Dokl. Akad. Nauk* **364**(1), 64-68 (in Russ.).

GRIFFIN, W.L., COUSENS, D.C., RYAN, C.S., SIE, S.H. & SUTER, G.F. (1989): Ni in chrome pyrope garnets: a new geothermometer. *Contrib. Mineral. Petrol*. **103**, 199-202.

_____, JAQUES, A.L., SIE, S.H., RYAN, C.G., COUSENS, D.R. & SUTER, G.F. (1988): Conditions of diamond growth: a proton microprobe study of inclusions in West Australian diamonds. *Contrib. Mineral. Petrol*. **99**,143-158.

_____ & RYAN, C.G. (1995): Trace elements in indicator minerals: area selection and target evaluation in diamond exploration. *J. Geochem. Explor*. **53**, 311-337.

GURNEY, J.J., HARRIS, J.W. & RICKARD, R.S. (1984): Silicate and oxide inclusions in diamonds from Orapa mine, Botswana. *In* Kimberlites II: The Mantle and Crust–Mantle Relationships (J. Kornprobst, ed.). Elsevier, Amsterdam, The Netherlands (3-9).

_____, _____, _____ & MOORE, R.O. (1985): Inclusions in Premier mine diamonds. *Trans. Geol. Soc. S. Afr.* **88**, 301-310.

HARTE, B. & HARRIS, J.W. (1994): Lower mantle mineral associations preserved in diamonds. *Mineral. Mag*. **58A**, 384-385.

_____, _____, HUTCHISON, M.T., WATT, G.R. & WILDING, M.C. (1999): Lower mantle mineral associations in diamonds from Sao Luiz, Brazil. *In* Mantle Petrology: Field Observations and High Pressure Experimentation: a Tribute to Francis R. (Joe) Boyd (Y. Fei, C.M. Bertka & B.O. Mysen, eds.). *Geochem. Soc., Spec. Publ.* **6**, 125-153.

JAQUES, A.L., HALL, A.E., SHERATON, J.W., SMITH, C.B., SUN, S.-S., DREW, R.M., FOUDOULIS, C. & ELLINGSEN, K. (1989): Composition of crystalline inclusions and C-isotopic composition of Argyle and Ellendale diamonds. *In* Kimberlites and Related Rocks. 2. Their Mantle/Crust Setting (J. Ross *et al*., eds.). *Geol. Soc. Aust., Spec. Publ.* **14**, 966-989.

KAMINSKY, F.V., BARTOSHINSKY, Z.V., BLINOVA, G.K., GALIMOV, E.M., GURKINA, G.A., KRASNIKOV, V.I., LAPUSHKOV, V.M., SOBOLEV, E.V. & SOBOLEV, N.V. (1988): *Comprehensive Study of Diamonds for Prospecting of Primary Deposits*. Moscow, Russia (in Russ.).

_____, ZAKHARCHENKO, O.D., DAVIES, R., GRIFFIN, W.L., KHACHATRYAN-BLINOVA, G.K. & SHIRYAEV, A.A. (2001): Superdeep diamonds from the Juina area, Mato Grosso State, Brazil. *Contrib. Mineral. Petrol*. (in press).

MCCANDLESS, T. E. & GURNEY, J. J. (1989): Sodium in garnet and potassium in clinopyroxene: criteria for classifying mantle eclogites. *In* Kimberlites and Related Rocks. 2. Their Mantle/Crust Setting (J. Ross *et al*., eds.). *Geol. Soc. Aust., Spec. Publ.* **14**, 827-832.

_____, LETENDRE, J. & EASTOE, C.J. (1999): Morphology and carbon isotope composition of microdiamonds from Dachine, French Guyana. *In* Proc. VIIth Int. Kimberlite Conf. **2** (J.J. Gurney, J.L. Gurney, M.D. Pascoe & S.H. Richardson, eds.). Red Roof Design, Cape Town, South Africa (550-556).

MENDOZA, V. (1972): Geologia del area Rio Suapure, Parte nordoccidental del escudo de Guyana, Estado Bolivar, Venezuela. *Memoria de la IX Conferenca Inter-Guayanas, Boletin de Geologia, Publ. Esp*. **6**, 306-338.

MENDELSSOHN, M.J. & MILLEDGE, H.J. (1995): Geologically significant information from routine analysis of the mid-infrared spectra of diamonds. *Int. Geol. Rev.* **37**, 95-110.

MEYER, H.O.A. (1982): Mineral inclusions in natural diamond. *In* Proc. Int. Gemological Symp., Santa Monica, California (445-465).

_____ & MCCALLUM, M.E. (1993): Diamonds and their sources in the Venezuelan portion of the Guyana Shield. *Econ. Geol.* **88**, 989-998.

_____ & SVISERO, D.P. (1975): Mineral inclusions in Brazilian diamonds. *Phys. Chem. Earth* **9**, 785-795.

NIXON, P.H. (1988): Diamond source rocks from Venezuela. *Indiaqua* **51**, 23-29.

_____, DAVIES, G.H., REX, D.C. & GRAY, A. (1992): Venezuela kimberlites. *In* Essays on Magmas and other Earth Fluids (a Volume in Appreciation of Professor P.G. Harris;

K.G. Cox & P.E. Baker, eds.). *J. Volcanol. Geotherm. Res.* **50**, 101-115.

_____, GRIFFIN, W.L., DAVIES, G.R. & CONDLIFFE, E. (1995): Cr garnet indicators in Venezuela kimberlites and their bearing on the evolution of the Guayana craton. *In* Kimberlites and Related Rocks **1** (H.O.A. Meyer & O.H. Leonardos, eds.). Brasilia, Brazil (378-387).

NORMAN, M.D., GRIFFIN, W.L., PEARSON, N.J., GARCIA, M.O. & O'REILLY, S.Y. (1998): Quantitative analysis of trace element abundances in glasses and minerals: a comparison of laser ablation inductively coupled plasma mass spectrometry, solution inductively coupled plasma mass spectrometry, proton microprobe and electron microprobe data. *J. Anal. Atomic Spectrom.* **13**, 477-482.

_____, PEARSON, N.J., SHARMA, A. & GRIFFIN, W.L. (1996): Quantitative analysis of trace elements in geological materials by laser ablation ICPMS: instrumental operating conditions and calibration values of NIST glasses. *Geostandards Newsletter* **20**, 247-261.

ORLOV, YU.L. (1987): *Mineralogy of Diamonds*. John Wiley & Sons, New York, N.Y.

OTTER, M.L., GURNEY, J.J. & MCCANDLESS, T.E. (1989): The carbon isotope composition of Sloan diamonds. *In* Workshop on Diamonds, 28th Int. Geol. Congress, Extended Abstr., 76-79.

REID, A.R. (1972): Stratigraphy of the type Area of the Roraima Group, Venezuela. *Memoria de la IX Conferenca Inter-Guayanas. Boletin de Geologia, Publ. Esp*. **6**.

ROBINSON, D.R., SCOTT, J.A., VAN NIEKERK, A. & ANDERSON, V.J. (1989): The sequence of events reflected in the diamonds of some southern African kimberlites. *In* Composition of Crystalline Inclusions and C-Isotopic Composition of Argyle and Ellendale Diamonds. *In* Kimberlites and Related Rocks. 2. Their Mantle/Crust Setting (J. Ross *et al*., eds.). *Geol. Soc. Aust., Spec. Publ.* **14**, 990-1000.

RYAN, C.G. & GRIFFIN, W.L. (1996): Garnet geotherms: pressure–temperature data from Cr-pyrope garnet xenocrysts in volcanic rocks. *J. Geophys. Res.* **101**, 5611-5625.

SCARRATT, K. (1992): Box A: a note on diamond types. *Gems & Gemmology, Spring issue*, 38-42.

SHIMIZU, N. & RICHARDSON, S.H. (1987): Trace element abundance patterns of garnet inclusions in peridotite-suite diamonds. *Geochim. Cosmochim. Acta* **51**, 755-758.

SIDDER, G.B. & MENDOZA, S.V. (1995): Geology of the Venezuelan Guayana Shield and its relation to the geology of the entire Guayana Shield. *U.S. Geol. Surv., Bull.* **2124**, B1-B41.

SIMAKOV, S.K. (1996): Garnet–pyroxene barometer for mantle eclogites. *Dokl. Akad. Nauk* **347**, 674-676 (in Russ.).

SOBOLEV, N.V., EFIMOVA, E.S., CHANNER, D.M.DER., ANDERSON, P.F.N. & BARRON, K.M. (1998): Unusual upper mantle beneath Guaniamo, Guyana Shield, Venezuela: evidence from diamond inclusions. *Geology* **26**, 971-974.

_____, GALIMOV, E.M., SMITH, C.B., YEFIMOVA, E.S., MALTSEV, K.A., HALL, E.E. & USOVA, L.V. (1989): Morphology, inclusions and carbon isotopic composition of diamonds from the King George alluvial deposit and the Argyle lamproitic pipe, Western Australia. *Geologiya i Geofizika*, No. 12, 3-18. (in Russ.).

SVISERO, D.P. & BAPTISTA, G.J. (1973): Inclusions en los diamantes de la Quebrada Grande, Distrito Cedeno, Estado Bolivar, Venezuela. *Second Congr. Lat. Amer. Geol.* (*Caracas*), *Resumenes*, 158-160.

TAYLOR, W.R, CANIL, D. & MILLEDGE, H.J. (1996): Kinetics of Ib to IaA nitrogen aggregation in diamonds. *Geochim. Comsmochim. Acta* **60**, 4725-4733.

ZAKHARCHENKO, O.D., KHARKIV, A.D., BOTOVA M.M., MAKHIN, A.I. & PAVLENKO, T.A. (1991): Inclusions of deep seated minerals in diamonds from kimberlite rocks of the north of the East-European Platform. *Mineral. Zh.* **13**(1), 42-52 (in Russ.).

Received April 5, 2000, revised manuscript accepted November 13, 2000.